NACA RM H56C30

NACA

RESEARCH MEMORANDUM

EFFECT OF SEVERAL WING MODIFICATIONS ON THE SUBSONIC AND TRANSONIC LONGITUDINAL HANDLING QUALITIES OF THE DOUGLAS D-558-II RESEARCH AIRPLANE

By Jack Fischel and Donald Reisert

High-Speed Flight Station
Edwards, Calif.

NATIONAL ADVISORY COMMITTEE
FOR AERONAUTICS

WASHINGTON
June 5, 1956
Declassified June 24, 1958

NACA RM H56C30

NATIONAL ADVISORY COMMITTEE FOR AERONAUTICS

RESEARCH MEMORANDUM

EFFECT OF SEVERAL WING MODIFICATIONS ON THE SUBSONIC AND TRANSONIC LONGITUDINAL HANDLING QUALITIES OF THE DOUGLAS D-558-II RESEARCH AIRPLANE

By Jack Fischel and Donald Reisert

SUMMARY

The subsonic and transonic longitudinal handling qualities of the Douglas D-558-II research airplane were measured with several wing modifications designed to alleviate swept-wing instability and pitch-up. The airplane configurations investigated included the basic wing configuration and two wing-fence configurations in combination with retracted, free-floating, or extended slats, and a wing leading-edge chord-extension configuration. All configurations were tested in the clean condition.

None of the wing modifications had an appreciable effect on the decay in stick-fixed stability (pitch-up) exhibited by the airplane at moderate angles of attack, and all configurations were considered by the pilots to be unsatisfactory and uncontrollable in the pitch-up region. Both flight and wind-tunnel results indicated that the position of the horizontal tail should be lowered appreciably to obtain substantial improvement in longitudinal handling qualities of the airplane.

Wing fences had no apparent effect on airplane buffeting characteristics with slats retracted. With wing slats free to float, the onset of buffeting was delayed at low Mach numbers, whereas buffeting was generally seriously aggravated by wing chord-extensions. Fully extending the wing slats had no appreciable effect on buffeting at low and moderate lifts but delayed the intensity rise to higher lift levels.

The variations and the values over the Mach number range of the apparent stability parameter $\frac{d\delta_e}{dC_N}$, the elevator control-force parameter $\frac{dF_e}{da_n}$, and the airplane normal-force-curve slope C_{N_α} were relatively unaffected by any of the wing modifications investigated. None of the

wing modifications had an appreciable effect on the trim-stability characteristics of the airplane, and all configurations exhibited similar trends over the test Mach number range.

INTRODUCTION

As part of the cooperative Air Force–Navy–NACA high-speed flight program, the National Advisory Committee for Aeronautics is conducting a flight research program at the High-Speed Flight Station, Edwards, Calif., utilizing the Douglas D-558-II swept-wing research airplane. During the course of this flight program, the effects of various modifications designed to alleviate swept-wing instability and pitch-up were investigated from stalling speed up to a maximum Mach number of about 1.0 (refs. 1 to 3). The various airplane configurations investigated are tabulated in table I and include the basic wing configuration and two wing-fence configurations in combination with retracted, free-floating, or extended slats, and a wing leading-edge chord-extension configuration. The low-speed stalling characteristics of the airplane in each of the previously mentioned configurations, with flaps and landing gear retracted and extended, are presented in reference 4. The subsonic and transonic longitudinal handling characteristics of the airplane in each of the configurations investigated are presented and compared in this paper.

SYMBOLS

a_n	normal acceleration, g units
b	wing span, ft
C_N	airplane normal-force coefficient, $\frac{a_n W}{qS}$
C_{N_α}	rate of change of airplane normal-force coefficient with angle of attack, $\frac{dC_N}{d\alpha}$, per deg
c	wing chord, ft
$\bar{c}$	mean aerodynamic chord of the wing, ft
$\frac{dF_e}{da_n}$	rate of change of elevator control force with normal acceleration, lb/g

$\frac{d\delta_e}{dC_N}$	rate of change of elevator position with airplane normal-force coefficient, deg
F_e	elevator control force, lb
g	acceleration due to gravity, ft/sec^2
h_p	pressure altitude, ft
i_t	stabilizer setting with respect to fuselage center line, positive when leading edge of stabilizer is up, deg
M	free-stream Mach number
q	free-stream dynamic pressure, lb/sq ft
S	wing area, sq ft
W	airplane weight, lb
α	angle of attack of airplane center line, deg
δ_e	elevator position with respect to stabilizer, deg

AIRPLANE

The Douglas D-558-II airplane used in this investigation is equipped with both a Westinghouse J34-WE-40 turbojet engine, which exhausts out the bottom of the fuselage between the wing and the tail, and a Reaction Motors, Inc. LR8-RM-6 rocket engine, which exhausts out the rear of the fuselage. The airplane is air-launched from a Boeing B-29 mother airplane. A photograph of the airplane is shown in figure 1 and a three-view drawing is shown in figure 2. Pertinent airplane dimensions and characteristics of the unmodified airplane are listed in table II.

For the present series of tests the basic clean-wing configuration and two wing-fence configurations were investigated in combination with a slat; an outboard wing leading-edge chord-extension was also investigated (table I). The fence configurations are shown in figures 3 and 4. The inboard wing fences were incorporated in the original airplane configuration to improve the longitudinal stability characteristics of the airplane at low speeds and at high angles of attack ($\alpha > 10^\circ$) when the wing slats were fully extended (ref. 5). The outboard wing fences were similar to the optimum fence configuration developed in the wind-tunnel investigation of reference 5 for improving the longitudinal stability

characteristics at high angles of attack in the airplane clean condition. The wing slats (figs. 5 and 6), may be locked in either the open (extended) or closed (retracted) position, or they may be unlocked (free floating). In the unlocked condition they are normally closed at low values of angle of attack or normal-force coefficient and open with increase in angle of attack. The left and right wing slats are interconnected and always have approximately the same position.

The wing leading-edge chord-extensions shown in figures 7 and 8 were similar to those tested in the wind tunnel and found to provide an improvement in static longitudinal stability at moderate angles of attack (refs. 6, 7, and unpublished data). The chord-extensions were approximately the NACA 63-008 airfoil profile in the streamwise direction and were faired into the wing profile over the span of the chord-extensions. In addition, the chord-extensions were faired into the wing tips and the inboard ends were flat-sided in the vertical streamwise plane. For this configuration the wing slats were locked closed and all fences were removed. Addition of the wing chord-extensions increased the wing area from 175 square feet to 181.2 square feet and the wing mean aerodynamic chord from 87.3 inches to 90.0 inches. For convenience in comparing these data with data for the unmodified airplane, however, all data presented are based on the dimensions of the unmodified airplane.

The airplane is equipped with an adjustable stabilizer, but there are no means provided for trimming out aileron or rudder-control forces. No aerodynamic balance or control-force boost system is used on any of the controls and longitudinal stick motion is linear with elevator motion. Hydraulic dampers installed on all control surfaces aid in preventing control-surface "buzz" and may influence stick forces at high control rates. Dive brakes are located on the rear portion of the fuselage.

INSTRUMENTATION

Among the standard NACA recording instruments installed in the airplane to obtain flight data were instruments which measured the following pertinent quantities:

Airspeed
Altitude
Angle of attack
Normal acceleration
Pitching velocity and acceleration
Stabilizer, elevator, and slat positions
Elevator control force

All instruments were synchronized by a common timer.

The elevator position was measured at the inboard end of the control surface, and the stabilizer position was measured at the plane of symmetry. All control positions were measured perpendicular to the control hinge line.

An NACA high-speed pitot-static tube (type A-6 of ref. 8) was mounted on a boom $4\frac{3}{4}$ feet forward of the nose of the airplane. The vane used to measure the angle of attack was mounted on the same boom about $3\frac{1}{2}$ feet forward of the nose of the airplane. Angles of attack are presented as measured with only instrument corrections applied. However, any inherent errors, such as caused by upwash effects, are believed to have a negligible effect on the analysis of the data. The possible Mach number errors are about ± 0.01 at $M < 0.8$ and about ± 0.02 at $M \approx 0.95$.

TESTS

The longitudinal handling qualities of the Douglas D-558-II airplane were measured with flaps and landing gear retracted in the airplane configurations listed in table I.

Longitudinal trim data ranging from $M \approx 0.6$ to $M \approx 1.1$ were obtained with the various airplane configurations during gradual climbs and level-flight speed runs at altitudes ranging from about 28,000 to 39,000 feet. Static longitudinal stability and control characteristics in accelerated flight were determined for each configuration during wind-up turns from a Mach number of about 0.4 to a Mach number of 1.0 in the altitude range from 10,300 to 38,500 feet. Data for the higher Mach numbers were generally obtained at the higher altitudes, and conversely. Except for the wing leading-edge chord-extension configuration, the airplane center-of-gravity locations ranged from 24.5 to 27.3 percent of the wing mean aerodynamic chord. For the chord-extension configuration, two conditions of airplane center-of-gravity location were employed, ranging from 22.6 to 24.7 and from 28.0 to 28.2 percent of the wing mean aerodynamic chord. (Only a few maneuvers were performed at the rearward center-of-gravity location, inasmuch as both the results obtained and the wind-tunnel results of refs. 5, 6, 7, and unpublished data indicated that the airplane had less static stability for a given center-of-gravity location when chord-extensions were installed. All remaining maneuvers with the chord-extensions were subsequently performed at the forward center-of-gravity location, which was selected to provide about the same static stability as existed with the unmodified airplane having its center of gravity at about 26 to 27 percent mean aerodynamic chord.)

At $M < 0.9$ the turns were performed using only the elevator, with the stabilizer remaining stationary during the maneuvers at settings ranging from about -0.2° to 3.6°. At $M > 0.9$, the turns were initiated using the elevator control with the stabilizer stationary; however, because of the decreased elevator effectiveness and accompanying large control forces at these speeds, use of stabilizer control was required during each maneuver to obtain higher lift levels and angles of attack.

PRESENTATION OF RESULTS

Representative stability data plots, illustrating the characteristics of each of the configurations of the D-558-II airplane during wind-up turns at various Mach numbers, are shown in figures 9 to 14 and, for convenience, are tabulated in table I. Some of these data were presented previously in references 1 to 3, and are reproduced in this paper, as measured, for illustrative purposes. As such, the data of figures 9 to 14 include the dynamic effects of pitching, therefore are not for static conditions, particularly at the higher angles of attack. To compare the stick-fixed stability data of the several configurations for comparable static conditions (zero pitching acceleration), representative variations of elevator position with angle of attack at two Mach numbers are shown in figure 15. The buffet boundaries of the various airplane configurations investigated are presented in figure 16. The low-lift stability parameters of the airplane in each of the several configurations are presented in figures 17 and 18, and the elevator trim characteristics are presented in figure 19. Relative elevator-stabilizer effectiveness characteristics over the test Mach number range are shown in figure 20.

DISCUSSION

High-Lift Characteristics

Pitch-up characteristics.- In general, the data of figures 9 to 14 indicate the airplane has reasonably linear stability (as exhibited by the variation of δ_e with α) and lift characteristics from low to moderate angles of attack. These characteristics become nonlinear at the higher values of α for all configurations. It may be observed in many of the maneuvers of figures 9 to 14 that, when C_N reached moderate values, the relative increase in α and C_N was greater than the increase in δ_e, indicating a decrease in stick-fixed stability and the onset of a pitch-up. In some instances, because the data of figures 9 to 14 are not corrected for pitching acceleration effects, the pitch-up

appears to be accentuated by the reversal of control and the continued increase in α and C_N. In other instances, after the initial decrease in stability and accompanying pitch-up, a retrimming effect is apparent, with the airplane regaining stability at higher angles of attack (for example, fig. 12(d)). These effects have been discussed in references 1 to 3 for most of the wing modifications tested and are, perhaps, more readily apparent when the data are corrected to static conditions (fig. 15). In general, none of the wing configurations provided tolerable behavior or measurable improvement compared with the basic wing configuration; however, some reduction in divergence rates was noted below a Mach number of 0.80 with slats extended and chord-extensions (fig. 15). Over a Mach number range from 0.8 to 0.95, all configurations were characterized by an abrupt change in stability at the pitch-up. At all speeds the pilots reported experiencing a lightening of the stick-force gradient prior to, or accompanying, the reduction in stick-fixed stability. The reduction in the stick-force gradient tended to aggravate the pitch-up tendency by allowing the pilot to increase the control rate with little or no additional effort.

Invariably, the pilots felt they had little or no control over the magnitude of the overshoot load factors once the pitch-up region was penetrated, and they tended to apply excessive corrective control to recover. As a result, in all configurations the pilots considered the airplane to be completely unsatisfactory and uncontrollable in the pitch-up region, particularly during combat-type maneuvers, and probably quite dangerous at the low altitudes. On the basis of wind-tunnel tests performed on a model of the D-558-II airplane (ref. 9), as well as other wind-tunnel and flight investigations, it has been concluded that with the present tail configuration of the D-558-II airplane (height above wing-chord plane extended is about $0.69\bar{c}$), a real cure of the pitch-up is not feasible. Lowering the horizontal tail to approximately the height of the wing-chord plane extended would be required to obtain substantial improvement in airplane longitudinal handling qualities.

Although some slight differences existed between the results for the various configurations, the values of C_N at which the stability decreased and pitch-up ensued varied from approximately 0.7 at $M = 0.5$ to approximately 0.6 at $M = 0.8$ and approximately 0.5 at $M = 0.95$. At $M > 0.95$ an abrupt increase in the values of C_N for pitch-up occurred and, generally, these values were attained only infrequently in the reported tests (refs. 1 to 3).

Buffet characteristics.- In general, the decrease in stability and the onset of pitch-up for each configuration were only slightly preceded by, or almost coincided with, the onset of buffeting of the airplane. The levels of C_N at which the onset of buffeting occurred are shown in figure 16 as a function of Mach number for all configurations except the slats-extended configuration. With the slats fully extended,

moderate buffeting appeared to exist over most of the lower and moderate lift range. It was found that the wing fences alone had no effect on the buffeting characteristics. Unlocking the wing slats tended to delay wing separation effects to higher lifts, thereby causing the onset of buffet to occur at higher lift levels for $M < 0.7$. The level of lift coefficients for the start of buffeting with wing chord-extensions was lowered somewhat below $M = 0.8$, compared with the unmodified airplane, and the pilot objected to the increase in buffet intensity, which was on the order of $\pm 0.5g$ at an altitude of about 30,000 feet. At $M < 0.85$, with either the chord-extension configuration or when the slats were retracted, the buffet-intensity rise occurred at a normal-force coefficient of about 0.05 above that for the onset of buffeting. When slats were unlocked (free floating) or fully extended, the increase in buffet intensity occurred quite gradually with increase in C_N, and the boundary for intensity rise varied from $C_N \approx 1.0$ at $M = 0.5$ to $C_N \approx 0.75$ at $M = 0.85$. In the transonic region above $M = 0.85$, the buffet intensity rise for all configurations occurred at $C_N \approx 0.5$, or greater.

In none of these configurations did the pilots consider the onset of buffeting to be an adequate warning of the impending pitch-up during an accelerated maneuver. Because of the alleviation in buffeting and in pitch-up divergence rates with slats fully extended, the pilots thought this modification provided the most improvement to the longitudinal handling characteristics of the airplane. Conversely, the pilots considered the chord-extension configuration to be the most objectionable, despite some alleviation in the pitch-up divergence rate, because of the severity of buffeting.

Low-Lift Characteristics

Stability parameters.- The variation of the airplane normal-force-curve slope C_{N_α} with Mach number for each of the configurations investigated is shown in figure 17. Within the accuracy of determination and within the scatter of C_{N_α} values shown, unlocking the wing slats had a negligible effect on C_{N_α} (figs. 17(a), (b), and (c)). The value of C_{N_α} for the basic wing configuration increased from approximately 0.065 at $M = 0.4$ to about 0.093 at $M = 0.9$, then decreased with further increase in Mach number.

Except for slight differences, the other configurations showed similar trends and values of C_{N_α} over the test Mach number range. A notable difference in the values of C_{N_α} can be observed at $M < 0.65$, where the two configurations with slats fully extended (figs. 17(d) and 17(e)) exhibited somewhat higher values than the other configurations investigated. The reasons for this effect are not apparent.

The variation of the apparent airplane stability parameter $\frac{d\delta_e}{dC_N}$ and the elevator control-force parameter $\frac{dF_e}{da_n}$ with Mach number for each of the configurations is shown in figure 18. For Mach numbers up to about $M = 0.7$, the values of $\frac{d\delta_e}{dC_N}$ and $\frac{dF_e}{da_n}$ of the basic wing configuration are substantially constant at about 10 and 12, respectively, (fig. 18(a)). At $M \gtrsim 0.7$, the values of both parameters increased rapidly with increase in Mach number, and at $M = 1.0$, $\frac{d\delta_e}{dC_N} \approx 60$ and $\frac{dF_e}{da_n} \approx 130$. In the variations with Mach number of both parameters, unlocking the wing slats produces no apparent effect. As discussed in reference 10 for the airplane configuration incorporating inboard fences on the unmodified wing, most of the increase in $\frac{d\delta_e}{dC_N}$ and $\frac{dF_e}{da_n}$ at $M \lesssim 0.85$ may be attributed to an increase in airplane stability, inasmuch as the change in elevator effectiveness is not appreciable in this range. At $M \gtrsim 0.85$, however, a large decrease in elevator effectiveness is expected as M increases, and reference 11 indicates appreciable increases in airplane stability in this range; therefore, the large increases noted in the apparent stick-fixed and stick-free parameters at $M \gtrsim 0.85$ probably result from these dual effects.

In general, little or no effect of modifying the basic wing configuration was shown by the variations of the apparent stick-fixed and stick-free stability parameters over the test Mach number range (fig. 18). The largest differences in the values of $\frac{d\delta_e}{dC_N}$ and $\frac{dF_e}{da_n}$ for the various configurations exist at the higher speeds, where the discrepancies appear to be aggravated by the rapid increases with Mach number of these two parameters. An almost constant difference in level of the values of $\frac{d\delta_e}{dC_N}$ is noted in figure 18(f) for the two ranges of center of gravity with the chord-extension configuration, and the data for the forward center-of-gravity location appear in better agreement with the data for the basic wing configuration. This effect was anticipated, since the investigation of references 6 and 7 indicated, for comparable center-of-gravity locations, the airplane with chord-extensions would exhibit slightly less stick-fixed stability than the unmodified airplane. A fairly complete discussion of the effects of the chord-extension on airplane stability was presented in reference 3.

An appreciable amount of the stability parameter data shown in this paper for the basic wing configuration and the inboard wing-fence configuration was also presented in reference 12 in which the data for the D-558-II airplanes being investigated were combined and presented for speeds up to $M \approx 2.0$. Since little difference was evident in the variations of $\frac{dC_N}{d\alpha}$, $\frac{d\delta_e}{dC_N}$, and $\frac{dF_e}{da_n}$ with M for the several configurations up to $M = 1.0$, it would appear the values and trends of these parameters at $M > 1.0$ would be similar to those shown in reference 12.

Trim characteristics.- The variation with Mach number of the elevator angle required to trim the airplane in each of the configurations investigated, for conditions of 1 g flight at an altitude of 35,000 feet and at a constant weight of 13,000 pounds, is shown in figure 19. By utilizing the values of $\frac{d\delta_e}{dC_N}$ shown for each configuration in figure 18, the original flight data obtained in each configuration were corrected to lift coefficients that would exist at the previously mentioned conditions.

The elevator trim curves for the basic wing configuration show the airplane has positive trim stability at $M \lesssim 0.82$ and a small neutrally stable region near $M \approx 0.85$ (fig. 19(a)). Starting at $M \approx 0.87$, as speed increased alternate airplane nose-down and nose-up trim changes occurred to $M = 1.03$, the maximum speed at which these data were obtained. For some stabilizer settings the trim changes were severe at $M \approx 1.0$.

Except for a slight difference in the magnitude of the values of δ_e required for trim at comparable stabilizer settings, the elevator trim curves for all configurations exhibited similar characteristics, thereby indicating similar trim stability. The differences in the magnitude of δ_e required for trim probably result from slight differences in airplane center of gravity for the several configurations, and also from possible slight differences in the wing center of pressure which resulted from the various wing modifications.

Although the trim data obtained on the subject D-558-II airplane were limited to subsonic and transonic speeds, similar data were obtained up to $M \approx 2.0$ on the all-rocket D-558-II airplane (basic wing configuration) and are reported in reference 12. Because the trim data obtained on both airplanes at subsonic and transonic speeds are in excellent agreement, and because all configurations investigated on the subject airplane exhibited similar characteristics, it is anticipated that all configurations investigated would have trim characteristics at supersonic speeds similar to those shown in reference 12.

Relative elevator-stabilizer effectiveness.- Figure 19(a) shows the change in the incremental elevator angle required for trim for a given change in stabilizer position as Mach number increased. Cross-plotting the data of figure 19(a) at given Mach numbers provided a measure of the change in the relative elevator-stabilizer effectiveness $\frac{di_t}{d\delta_e}$ which is shown in figure 20 as a function of Mach number for the basic wing configuration. Although both controls tend to lose effectiveness at transonic speeds, it is evident from figure 20 that the loss in elevator effectiveness is much greater than the comparable loss in stabilizer effectiveness as M increases. This loss in elevator effectiveness is serious, since it necessitates the use of appreciably larger control deflections for trim and maneuvering in the transonic region, and tends to limit the maneuverability of the airplane. (See data at $M > 0.9$, figs. 9 to 14.)

Although sufficient trim-stability data were not obtained for each of the configurations to determine the individual relative elevator-stabilizer effectiveness, the relative agreement in all data obtained suggests the trends shown for $\frac{di_t}{d\delta_e}$ in figure 20 for the basic wing configuration would also hold true for each of the wing modifications investigated.

Also shown in figure 20 are the variations with Mach number of $\frac{di_t}{d\delta_e}$ obtained in other tests of the D-558-II airplane in either the basic wing configuration (ref. 12) or the inboard wing-fence configuration (ref. 10). The values of $\frac{di_t}{d\delta_e}$ from reference 10 were obtained from elevator trim stability curves, similar to the method used in the subject tests, for dives from 25,000 to 15,000 feet. The values of $\frac{di_t}{d\delta_e}$ from reference 12 were obtained from elevator and stabilizer maneuvers (pull-ups and wind-up turns) at altitudes generally in excess of 35,000 feet. The agreement shown in figure 20 for the values of $\frac{di_t}{d\delta_e}$ over the test Mach number range is good. The small discrepancies shown may be attributed to the technique and operating conditions under which these data were obtained, and to the accuracy of determination.

CONCLUSIONS

Results of a longitudinal handling qualities investigation at subsonic and transonic speeds of the swept-wing Douglas D-558-II research airplane, in the basic clean-wing configuration and with various wing modifications designed to alleviate swept-wing instability and pitch-up, led to the following conclusions:

1. None of the wing modifications had an appreciable effect on the decay in stick-fixed stability (pitch-up) exhibited by the airplane at moderate angles of attack, particularly over a Mach number range from about 0.8 to 0.95. All configurations were considered unsatisfactory and uncontrollable in the pitch-up region by the pilots. On the basis of these tests and other flight and tunnel investigations, it is felt the position of the horizontal tail on this airplane should be lowered appreciably to obtain substantial improvement in longitudinal handling qualities.

2. Wing fences had no apparent effect on the buffeting characteristics with slats retracted; however, unlocking the wing slats raised the buffet boundary, below a Mach number of 0.70, above that for the retracted slats condition for the basic-wing, one-fence, and two-fence configurations. Wing chord-extensions lowered the buffet boundary, compared with the unmodified airplane configuration, up to a Mach number of 0.80 and caused an increase in buffet intensity which was objectionable to the pilot. Moderate buffeting appeared to exist over most of the lower and moderate lift range with the slats fully extended; however, this configuration did alleviate some of the pitch-up divergence rate and appeared to the pilots to provide the greatest improvement in the longitudinal handling characteristics of the airplane.

3. At low lift coefficients, the trends in the values of the apparent stability parameter $\frac{d\delta_e}{dC_N}$ and the elevator control-force parameter $\frac{dF_e}{da_n}$ were relatively unaffected by any of the wing modifications investigated. The values of $\frac{d\delta_e}{dC_N}$ increased by a factor of about 6 and the values of $\frac{dF_e}{da_n}$ increased by a factor of about 11 as Mach number increased from 0.5 to 1.0.

4. The variation with Mach number of the airplane normal-force-curve slope C_{N_α} was little affected by wing modification. Values of C_{N_α} increased from about 0.065 at a Mach number of 0.4 to about 0.093 at a Mach number of 0.9, then decreased with further increase in Mach number.

5. None of the wing modifications had an appreciable effect on the trim-stability characteristics of the airplane and all configurations exhibited similar trends over the Mach number range. The airplane was stable at Mach numbers below about 0.82, and exhibited characteristic nose-down and nose-up trim changes between Mach numbers of about 0.87 and 1.03.

6. The loss in elevator effectiveness in the transonic speed range is appreciably greater than the comparable loss in stabilizer effectiveness. The relative elevator-stabilizer control-effectiveness parameter $\frac{di_t}{d\delta_e}$ decreased from a value of about 0.43 at a Mach number of 0.6 to less than 0.2 at a Mach number of 1.0.

High-Speed Flight Station,
National Advisory Committee for Aeronautics,
Edwards, Calif., March 22, 1956.

REFERENCES

1. Fischel, Jack, and Nugent, Jack: Flight Determination of the Longitudinal Stability in Accelerated Maneuvers at Transonic Speeds for the Douglas D-558-II Research Airplane Including the Effects of an Outboard Wing Fence. NACA RM L53A16, 1953.

2. Fischel, Jack: Effect of Wing Slats and Inboard Wing Fences on the Longitudinal Stability Characteristics of the Douglas D-558-II Research Airplane in Accelerated Maneuvers at Subsonic and Transonic Speeds. NACA RM L53L16, 1954.

3. Fischel, Jack, and Brunn, Cyril D.: Longitudinal Stability Characteristics in Accelerated Maneuvers at Subsonic and Transonic Speeds of the Douglas D-558-II Research Airplane Equipped With a Leading-Edge Wing Chord-Extension. NACA RM H54H16, 1954.

4. Fischel, Jack, and Reisert, Donald: Effect of Several Wing Modifications on the Low-Speed Stalling Characteristics of the Douglas D-558-II Research Airplane. NACA RM H55E31a, 1955.

5. Queijo, M. J., and Jaquet, Byron M.: Wind-Tunnel Investigation of the Effect of Chordwise Fences on Longitudinal Stability Characteristics of an Airplane Model With a 35° Sweptback Wing. NACA RM L50K07, 1950.

6. Jaquet, Byron M.: Effects of Chord Discontinuities and Chordwise Fences on Low-Speed Static Longitudinal Stability of an Airplane Model Having a 35° Sweptback Wing. NACA RM L52C25, 1952.

7. Jaquet, Byron M.: Effects of Chord-Extension and Droop of Combined Leading-Edge Flap and Chord-Extension on Low-Speed Static Longitudinal Stability Characteristics of an Airplane Model Having a 35° Sweptback Wing With Plain Flaps Neutral or Deflected. NACA RM L52K21a, 1953.

8. Gracey, William, Letko, William, and Russell, Walter R.: Wind-Tunnel Investigation of a Number of Total-Pressure Tubes at High Angles of Attack - Subsonic Speeds. NACA TN 2331, 1951. (Supersedes NACA RM L50G19.)

9. Queijo, M. J., and Wolhart, Walter D.: Wind-Tunnel Investigation of the Effects of Horizontal-Tail Position on the Low-Speed Longitudinal Stability Characteristics of an Airplane Model With a 35° Sweptback Wing Equipped With Chordwise Fences. NACA RM L51H17, 1951.

10. Sjoberg, S. A., Peele, James R., and Griffith, John H.: Flight Measurements With the Douglas D-558-II (BuAero No. 37974) Research Airplane. Static Longitudinal Stability and Control Characteristics at Mach Numbers Up to 0.87. NACA RM L50K13, 1951.

11. Silvers, H. Norman, and King, Thomas J., Jr.: Investigation at High Subsonic Speeds of the Effects of Various Underwing External-Store Arrangements on the Aerodynamic Characteristics of a 1/16-Scale Model of the Douglas D-558-II Research Airplane. NACA RM L55D11, 1955.

12. Ankenbruck, Herman O.: Determination of Longitudinal Handling Qualities of the D-558-II Research Airplane at Transonic and Supersonic Speeds to a Mach Number of About 2.0. NACA RM H54G29a, 1954.

TABLE I

INDEX OF AIRPLANE CONFIGURATIONS INVESTIGATED

Airplane configuration	Location of center of gravity	Figures showing configuration	Figures showing basic data for configuration
Basic wing (no fences)			
Slats retracted (locked closed)	0.249$\bar{c}$ to 0.273$\bar{c}$	2, 5	9(a), (b), (c), (d)
Slats unlocked	0.245$\bar{c}$ to 0.259$\bar{c}$		9(e), (f)
Inboard wing fences			
Slats retracted	0.251$\bar{c}$ to 0.261$\bar{c}$	1, 3	10(a), (b), (c), (d)
Slats unlocked	0.25$\bar{c}$		10(e), (f)
Inboard and outboard wing fences			
Slats retracted	0.246$\bar{c}$ to 0.262$\bar{c}$	3, 4	11(a), (b), (c)
Slats unlocked	0.266$\bar{c}$ to 0.267$\bar{c}$		11(d)
Wing slats fully extended (no wing fences)	0.252$\bar{c}$ to 0.269$\bar{c}$	5	12(a), (b), (c), (d)
Wing slats fully extended and inboard wing fences	0.254$\bar{c}$ to 0.266$\bar{c}$	5, 6	13(a), (b), (c), (d)
Wing leading-edge chord-extensions (no fences, slats retracted)	0.226$\bar{c}$ to 0.247$\bar{c}$ 0.280$\bar{c}$ to 0.282$\bar{c}$	7, 8	14(a), (b)

TABLE II

PHYSICAL CHARACTERISTICS OF THE UNMODIFIED

DOUGLAS D-558-II AIRPLANE

Wing:	
Root airfoil section (normal to 0.30 chord of unswept panel)	NACA 63-010
Tip airfoil section (normal to 0.30 chord of unswept panel)	NACA 63$_1$-012
Total area, sq ft	175.0
Span, ft	25.0
Mean aerodynamic chord, in.	87.301
Root chord (parallel to plane of symmetry), in.	108.51
Tip chord (parallel to plane of symmetry), in.	61.18
Taper ratio	0.565
Aspect ratio	3.570
Sweep at 0.30 chord of unswept panel, deg	35.0
Sweep of leading edge, deg	38.8
Incidence at fuselage center line, deg	3.0
Dihedral, deg	-3.0
Geometric twist, deg	0
Total aileron area (rearward of hinge line), sq ft	9.8
Aileron travel (each), deg	±15
Total flap area, sq ft	12.58
Flap travel, deg	50
Horizontal tail:	
Root airfoil section (normal to 0.30 chord of unswept panel)	NACA 63-010
Tip airfoil section (normal to 0.30 chord of unswept panel)	NACA 63-010
Area (including fuselage), sq ft	39.9
Span, in.	143.6
Mean aerodynamic chord, in.	41.75
Root chord (parallel to plane of symmetry), in.	53.6
Tip chord (parallel to plane of symmetry), in.	26.8
Taper ratio	0.50
Aspect ratio	3.59
Sweep at 0.30 chord line of unswept panel, deg	40.0
Dihedral, deg	0
Elevator area, sq ft	9.4
Elevator travel, deg	
Up	25
Down	15
Stabilizer travel, deg	
Leading edge up	4
Leading edge down	5
Vertical tail:	
Airfoil section (normal to 0.30 chord of unswept panel)	NACA 63-010
Area, sq ft	36.6
Height from fuselage center line, in.	98.0
Root chord (parallel to fuselage center line), in.	146.0
Tip chord (parallel to fuselage center line), in.	44.0
Sweep angle at 0.30 chord of unswept panel, deg	49.0
Rudder area (rearward of hinge line), sq ft	6.15
Rudder travel, deg	±25
Fuselage:	
Length, ft	42.0
Maximum diameter, in.	60.0
Fineness ratio	8.40
Speed-retarder area, sq ft	5.25
Engines:	
Turbojet	J34-WE-40
Rocket	LR8-RM-6
Airplane weight, lb:	
Full jet and rocket fuel	15,570
Full jet fuel	12,382
No fuel	10,822

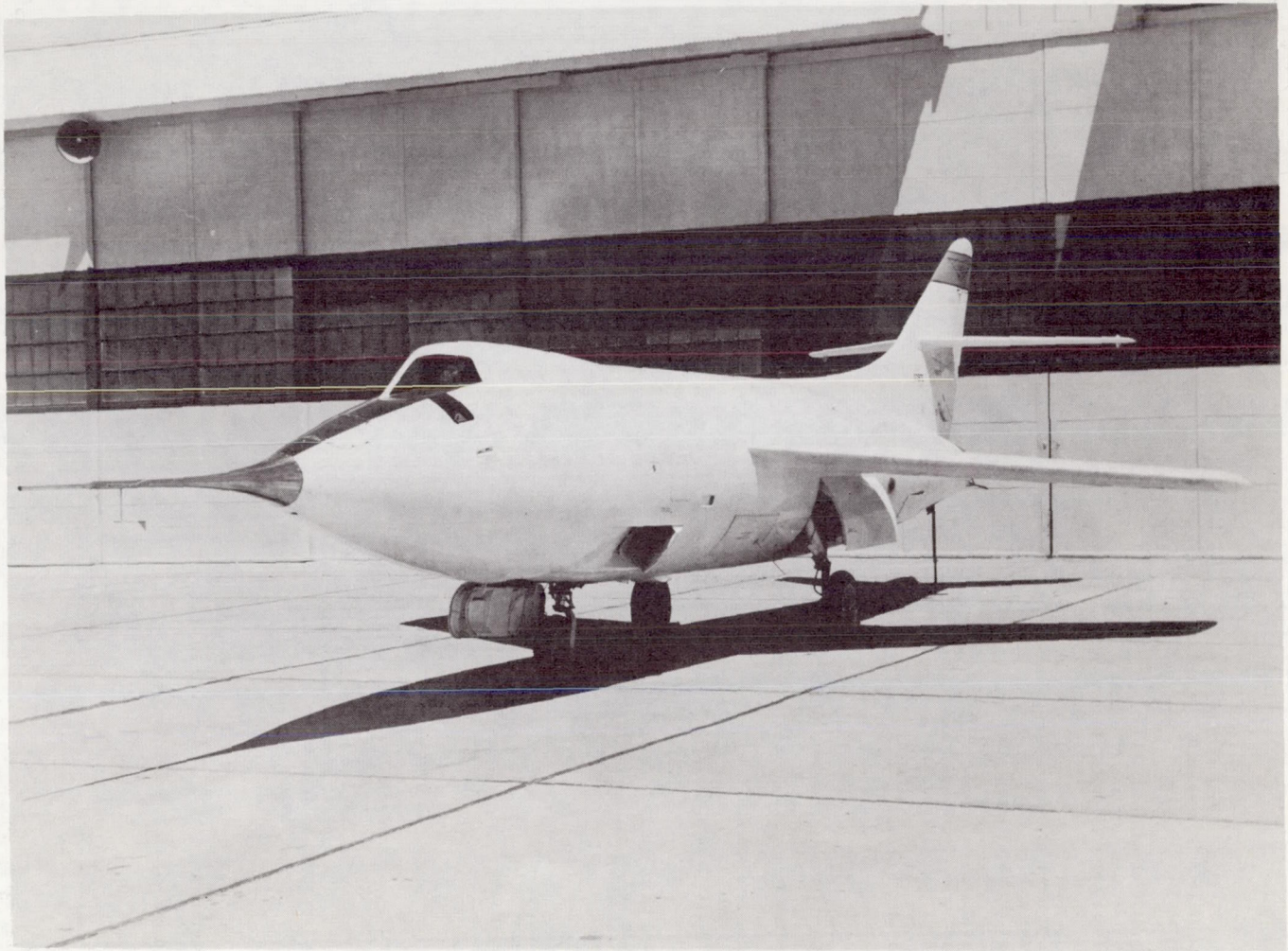

E-488

Figure 1.- Three-quarter front view of Douglas D-558-II airplane. Inboard fences shown installed on wing.

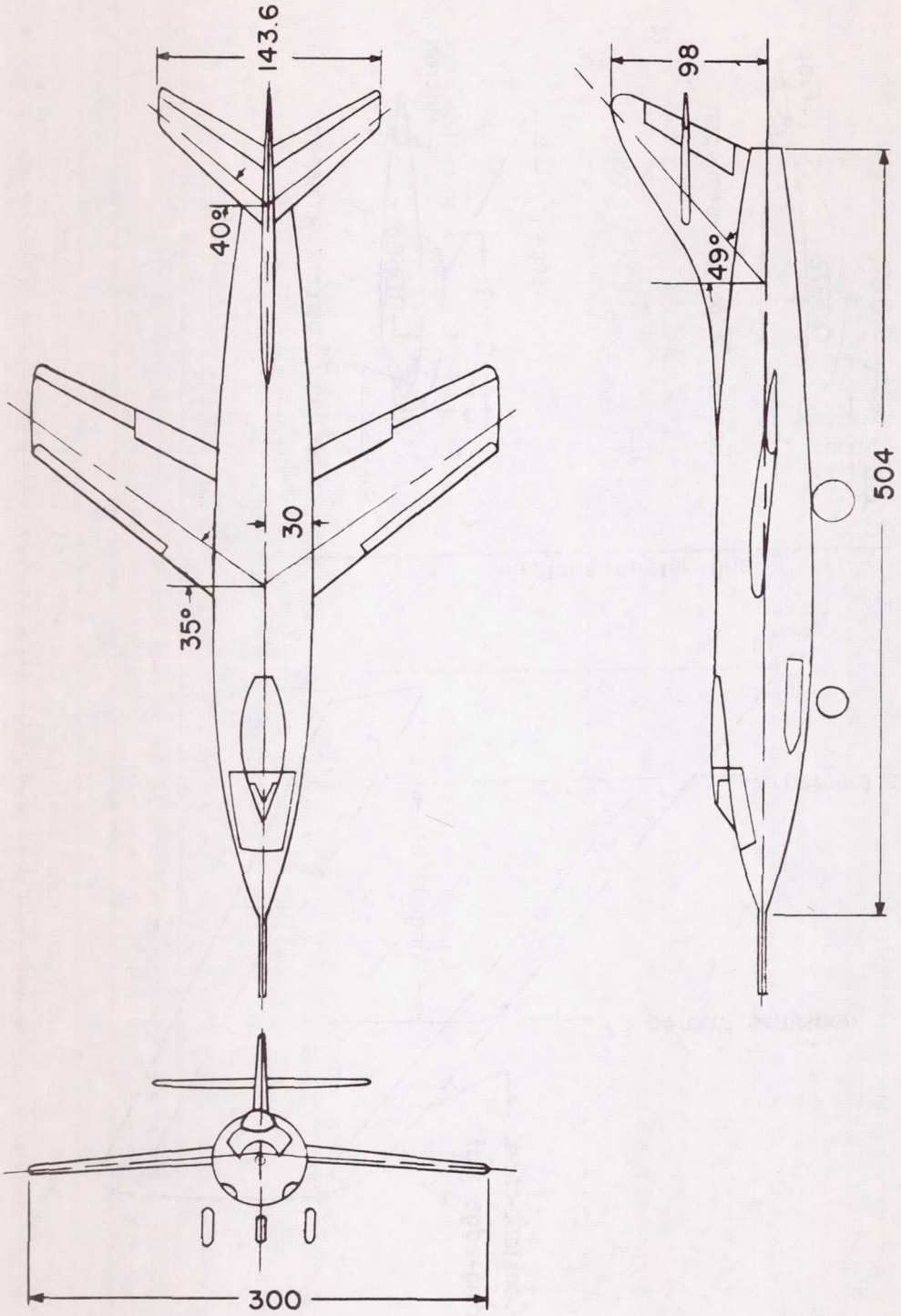

Figure 2.- Three-view drawing of the Douglas D-558-II research airplane. All dimensions in inches.

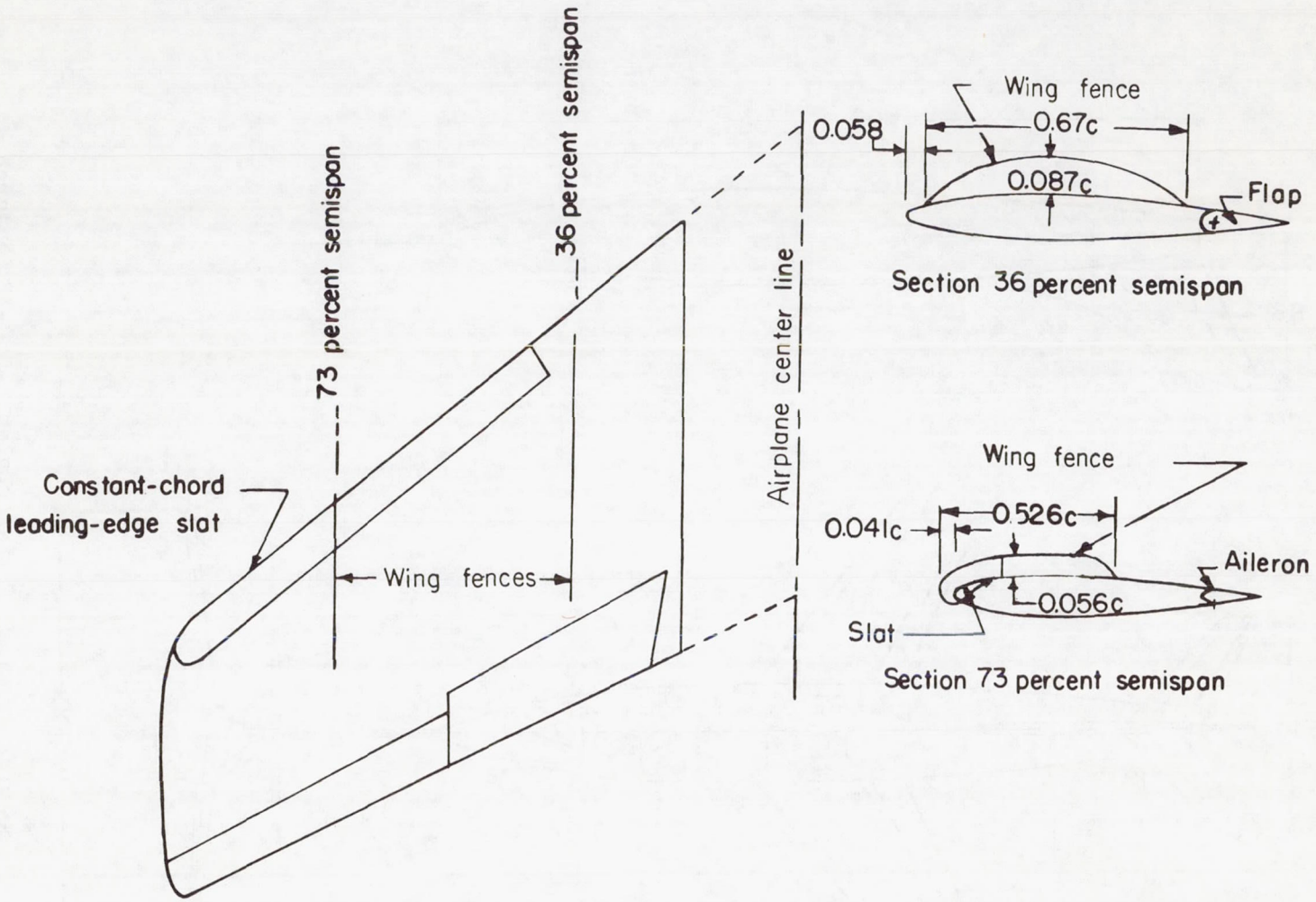

Figure 3.- Plan form and sections of the wing of the D-558-II airplane showing the location and shape of wing fences (stall-control vanes) used in the investigation.

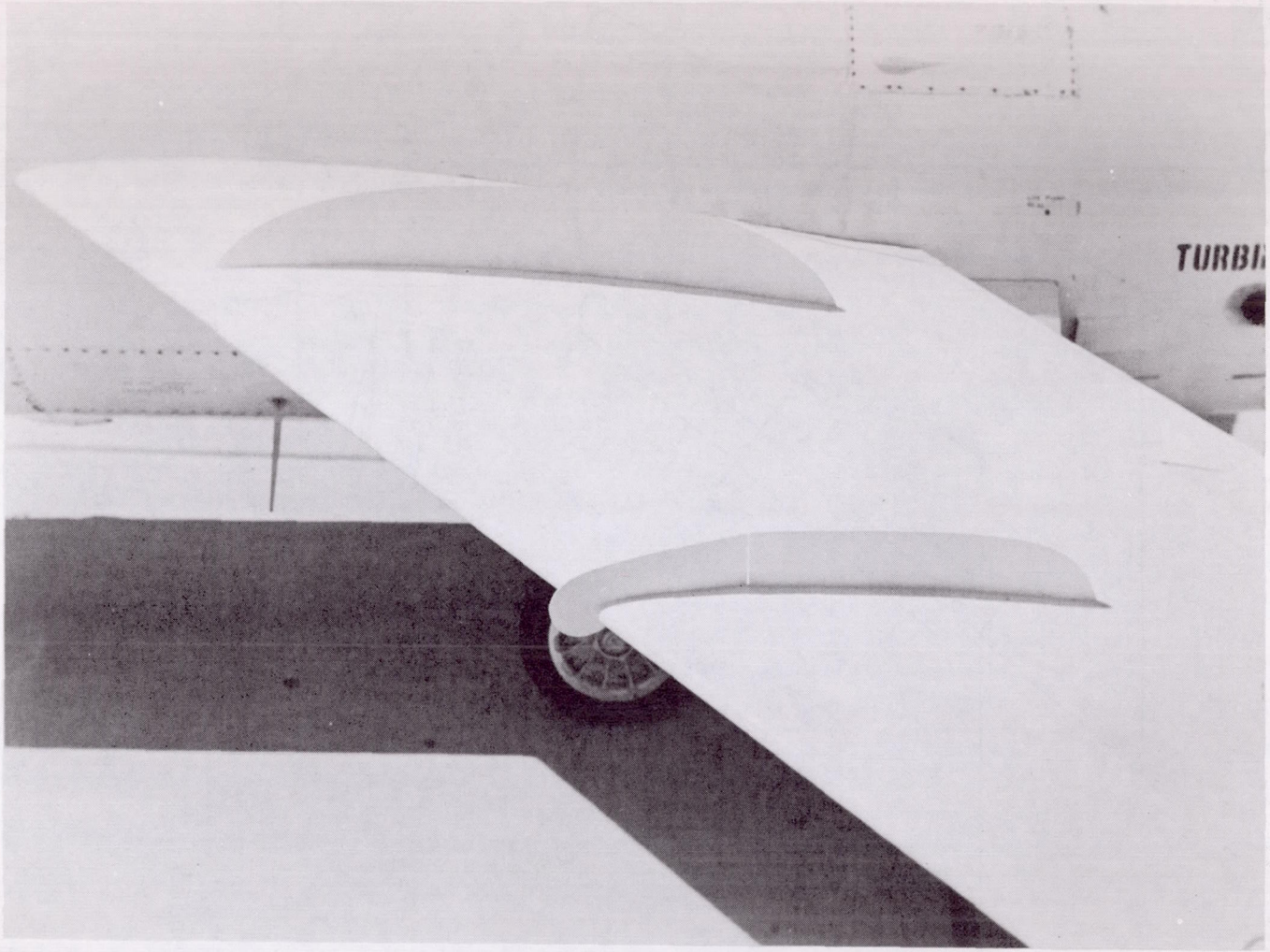

E-584

Figure 4.- Photograph of the D-558-II wing, showing the inboard and outboard fences (stall-control vanes) on the wing.

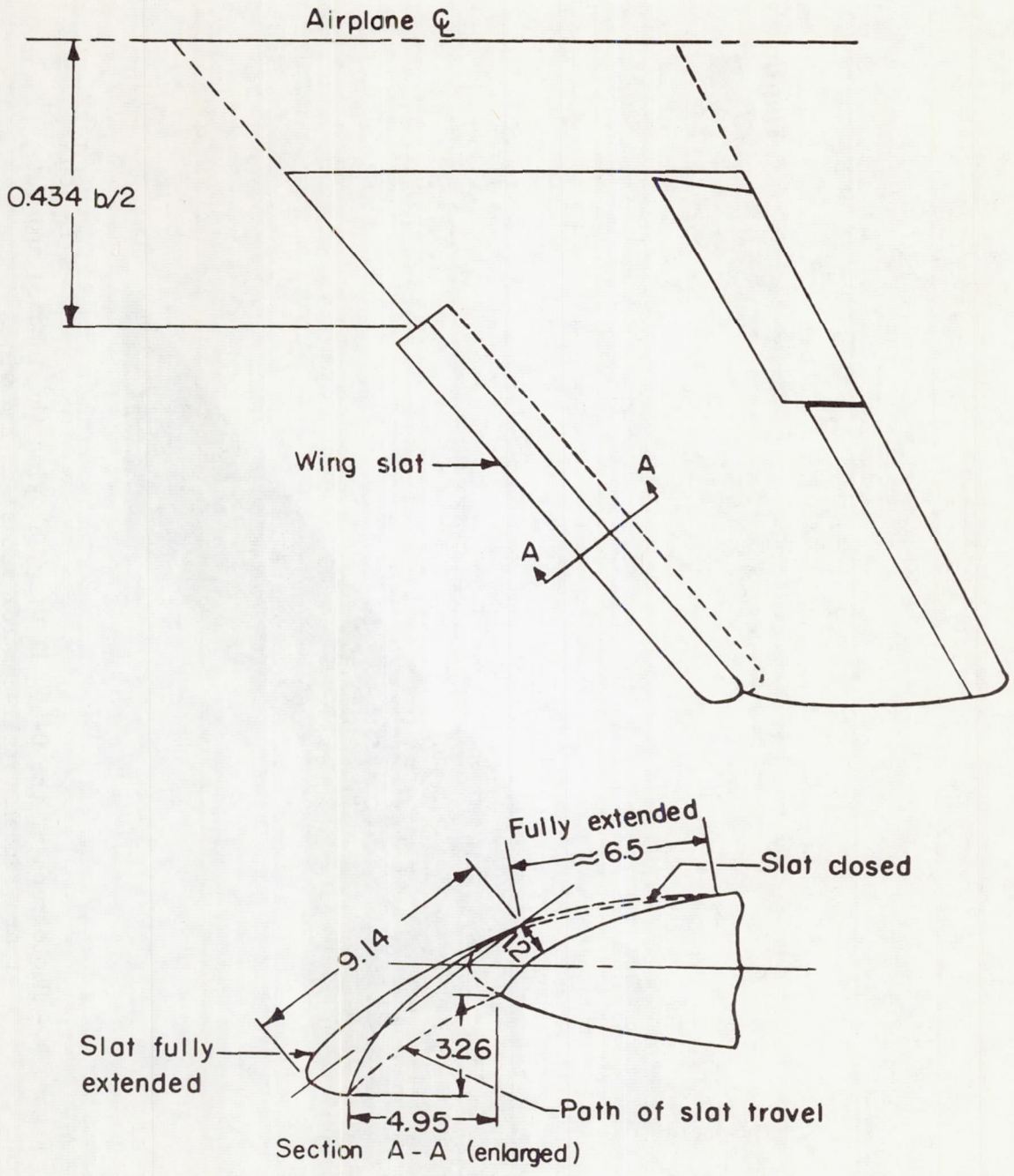

Figure 5.- Plan form and sections of the wing of the D-558-II airplane showing details of the wing slat in the retracted and extended positions.

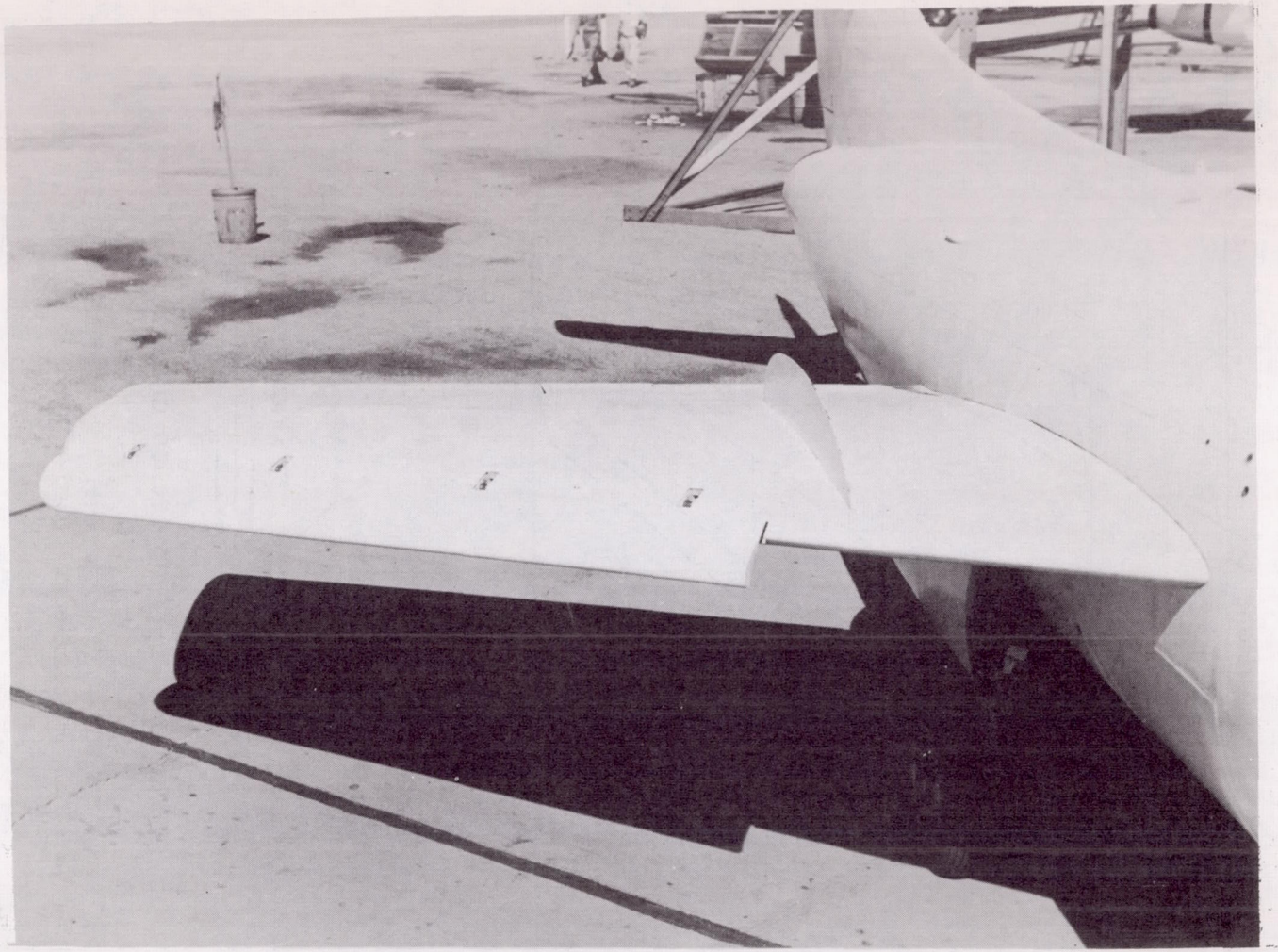

E-817

Figure 6.- Photograph of right wing of D-558-II airplane showing slat in fully extended position and inboard fence on wing.

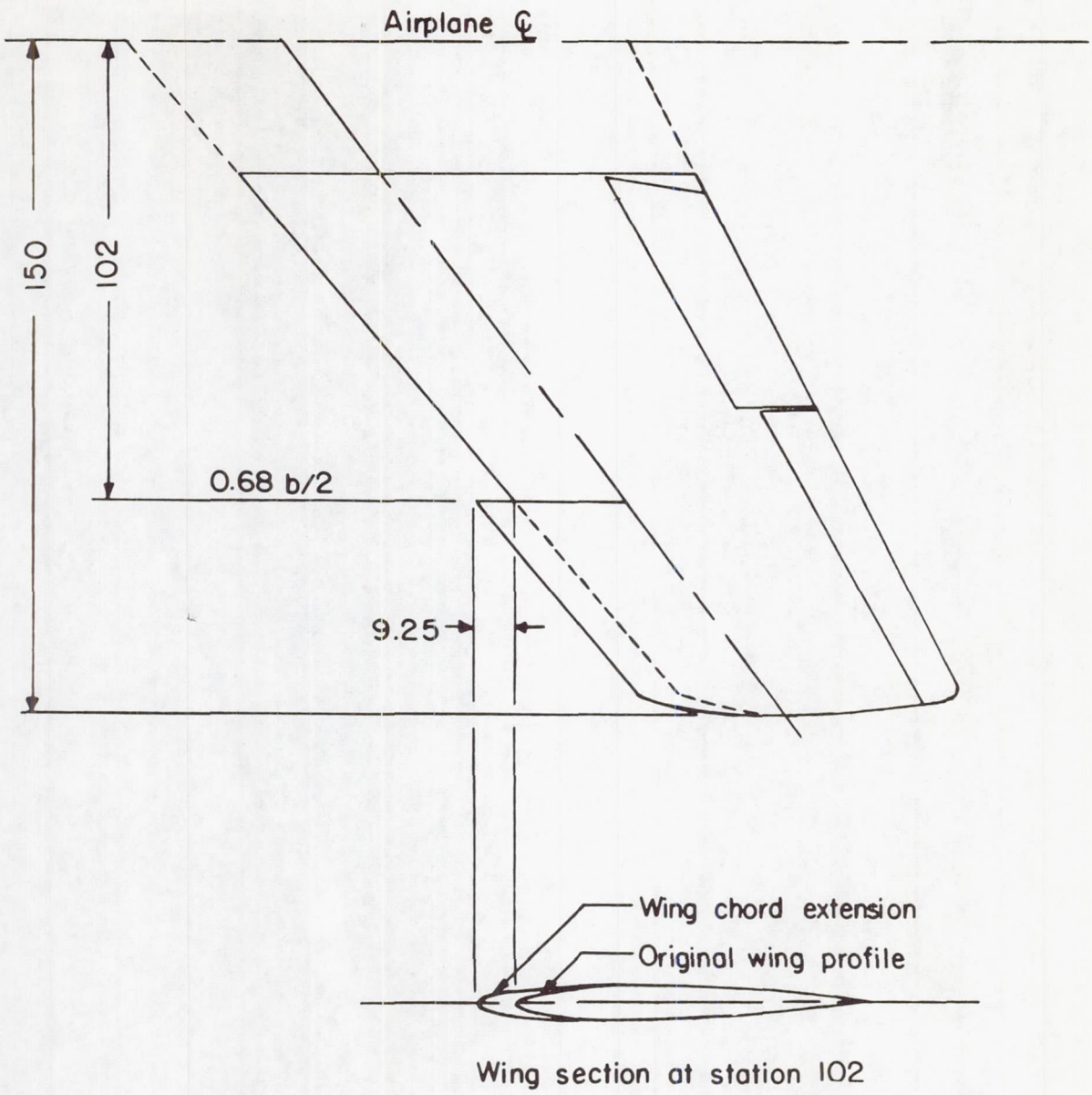

Figure 7.- Plan form and section of the wing of the D-558-II airplane showing the wing leading-edge chord-extension configuration.

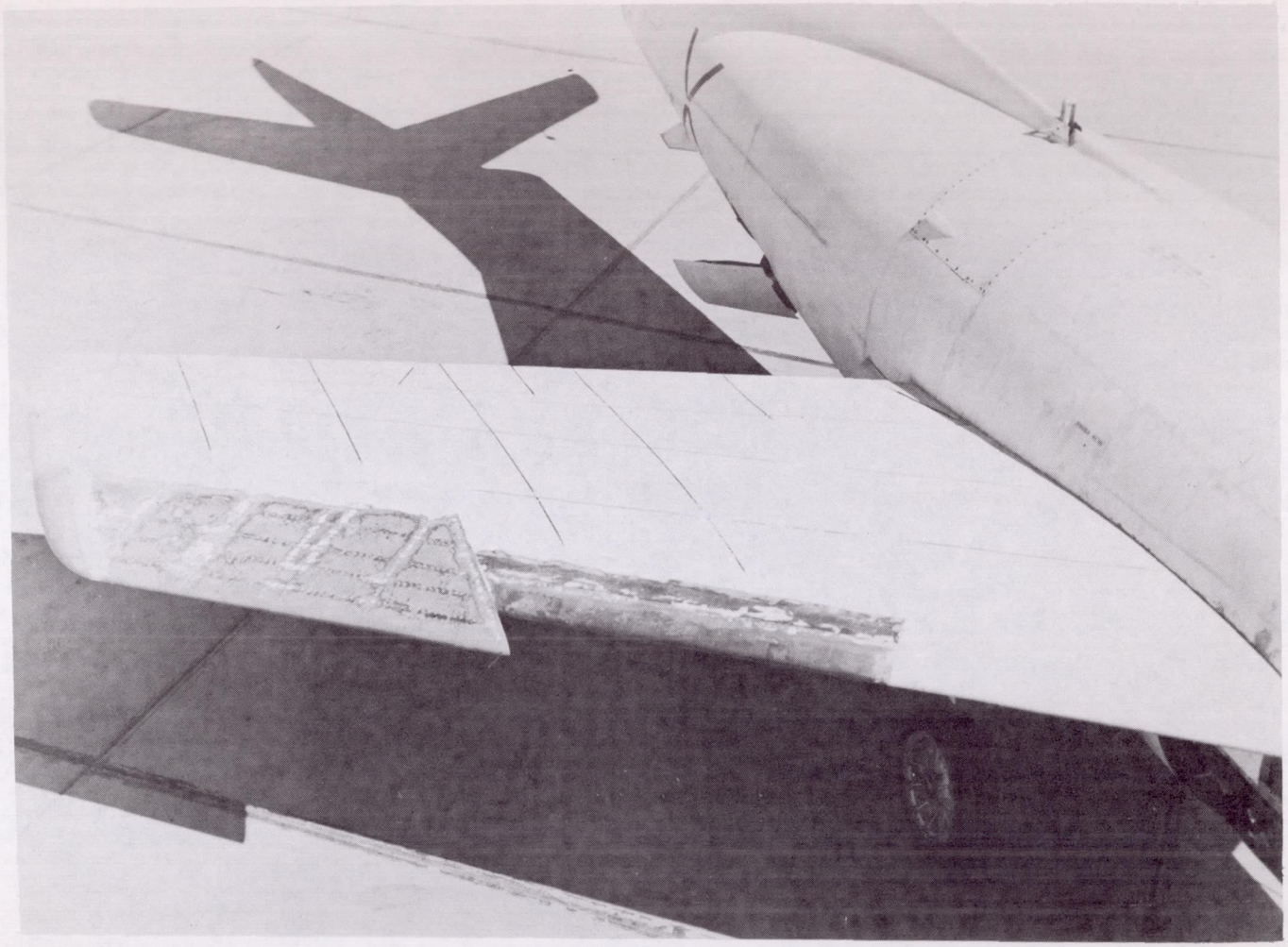

E-927

Figure 8.- Photograph of the wing of the D-558-II airplane showing the wing leading-edge chord-extension configuration.

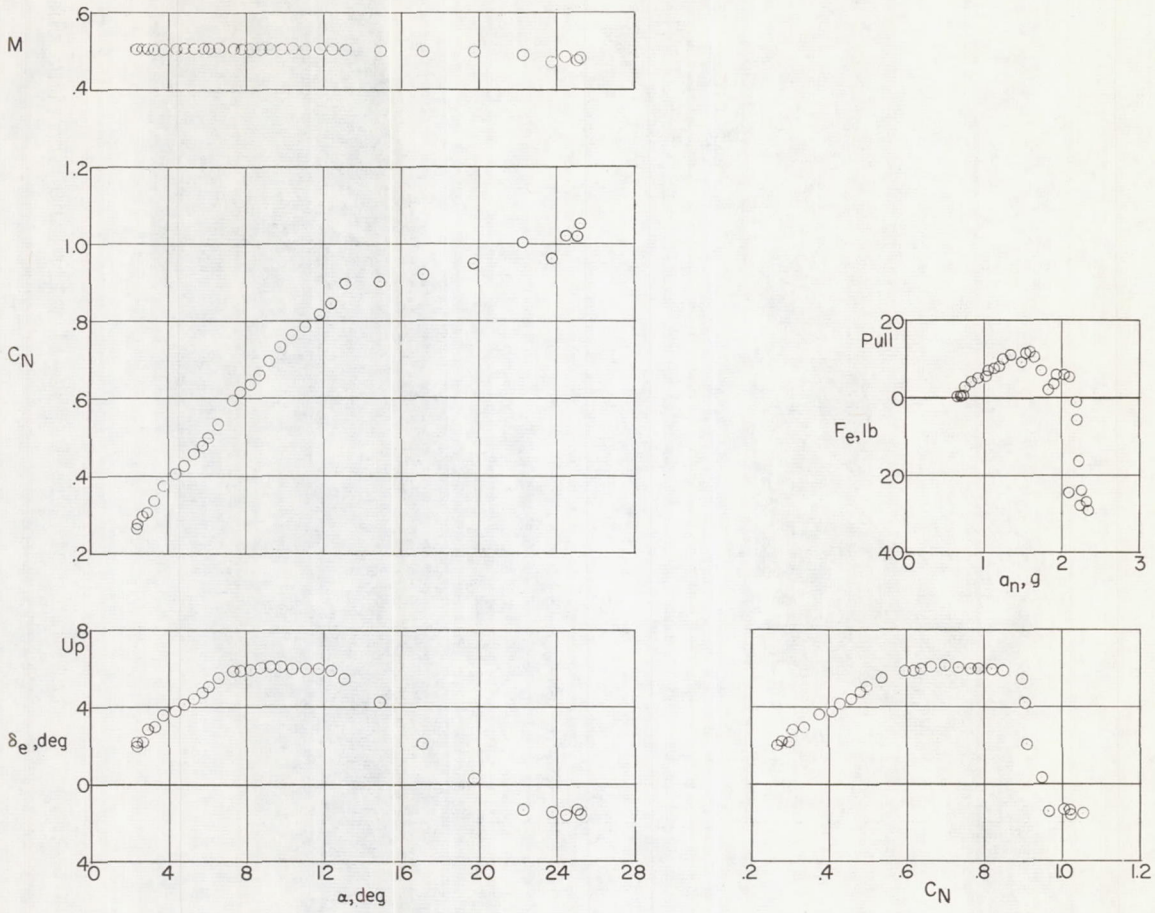

(a) $h_p \approx 22{,}000$ feet; $i_t = 1.6^\circ$; center of gravity at $0.268\bar{c}$; slats retracted.

Figure 9.- Static longitudinal stability characteristics of the Douglas D-558-II research airplane in turning flight. Basic wing configuration.

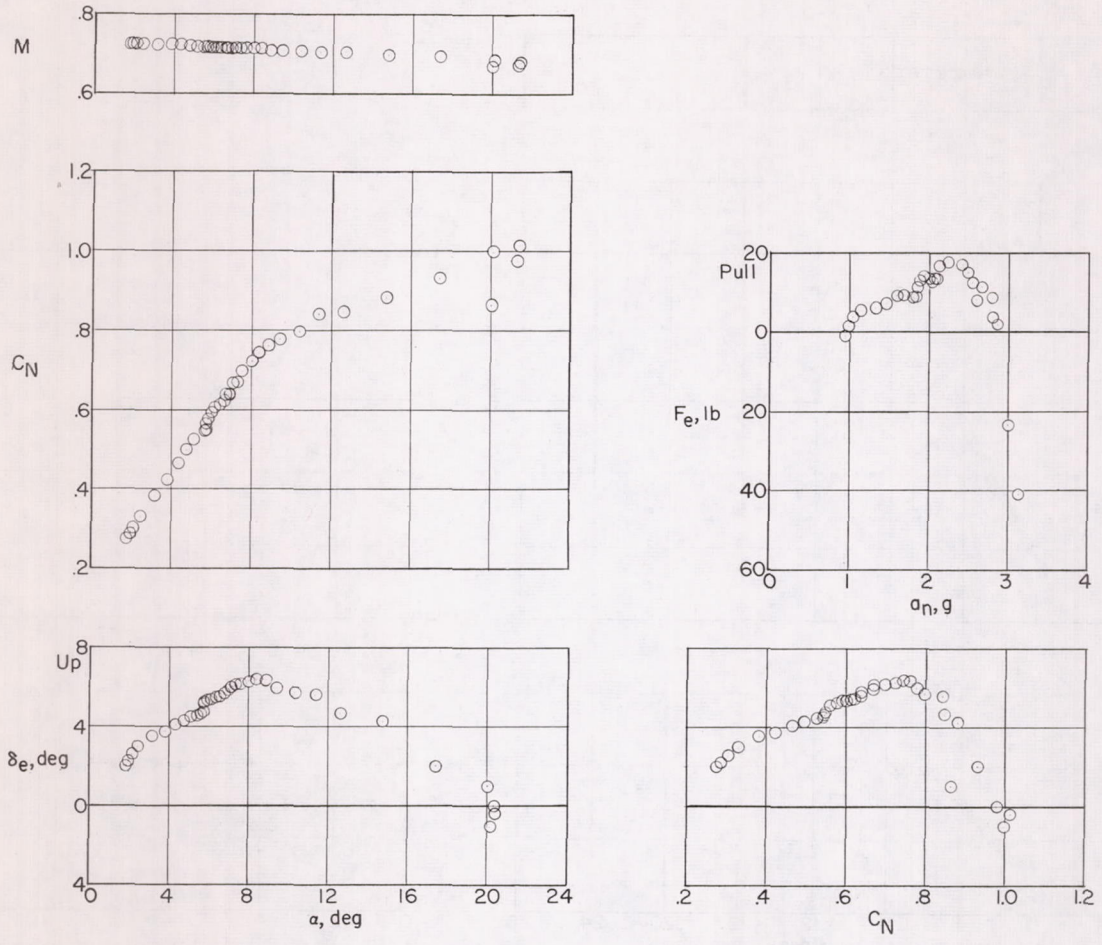

(b) $h_p \approx 29,800$ feet; $i_t = 1.6^\circ$; center of gravity at $0.262\bar{c}$; slats retracted.

Figure 9.- Continued.

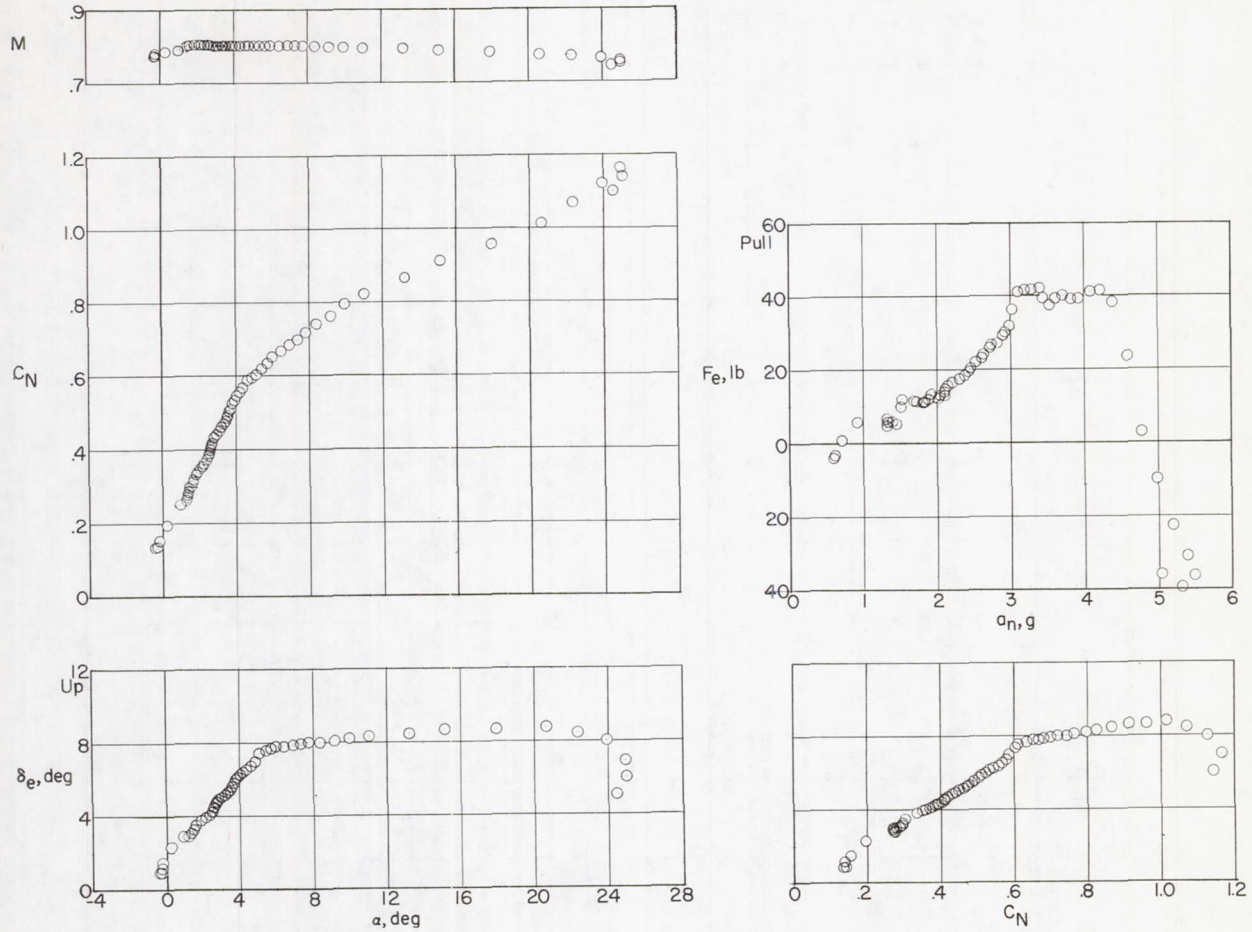

(c) $h_p \approx 25{,}900$ feet; $i_t = 2.1^\circ$; center of gravity at $0.249\bar{c}$; slats retracted.

Figure 9.- Continued.

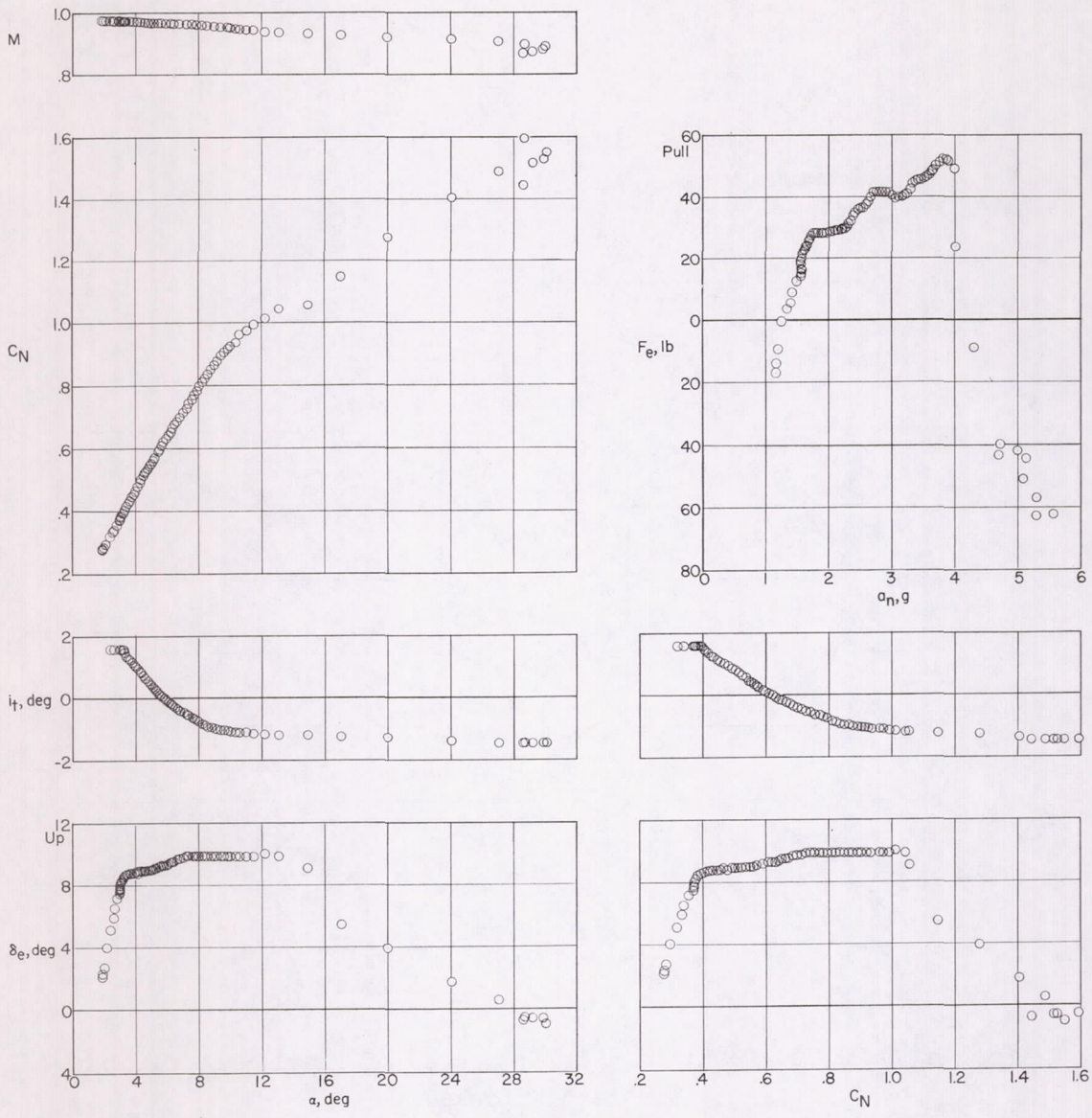

(d) $h_p \approx 37,200$ feet; center of gravity at $0.272\bar{c}$; slats retracted.

Figure 9.- Continued.

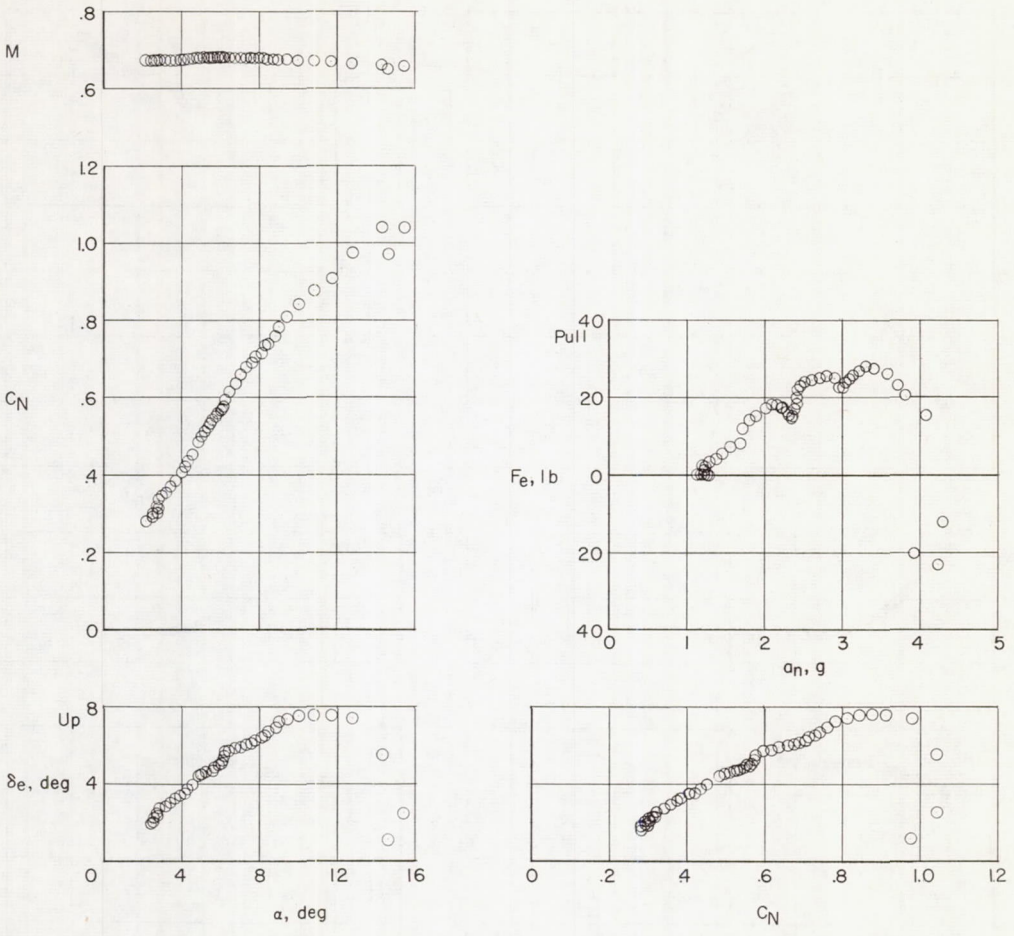

(e) $h_p \approx 22{,}700$ feet; $i_t = 1.7^\circ$; center of gravity at $0.253\bar{c}$; slats unlocked.

Figure 9.- Continued.

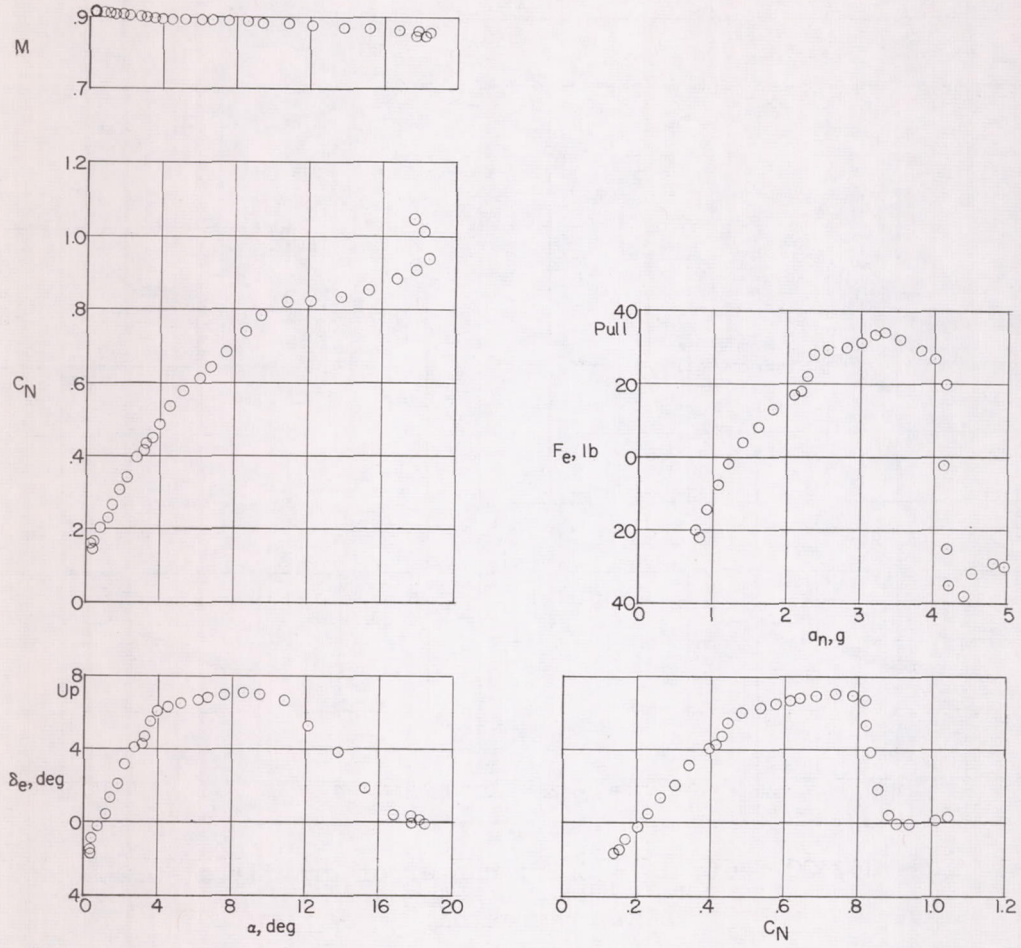

(f) $h_p \approx 29{,}800$ feet; $i_t = 1.2^\circ$; center of gravity at $0.249\bar{c}$; slats unlocked.

Figure 9.- Concluded.

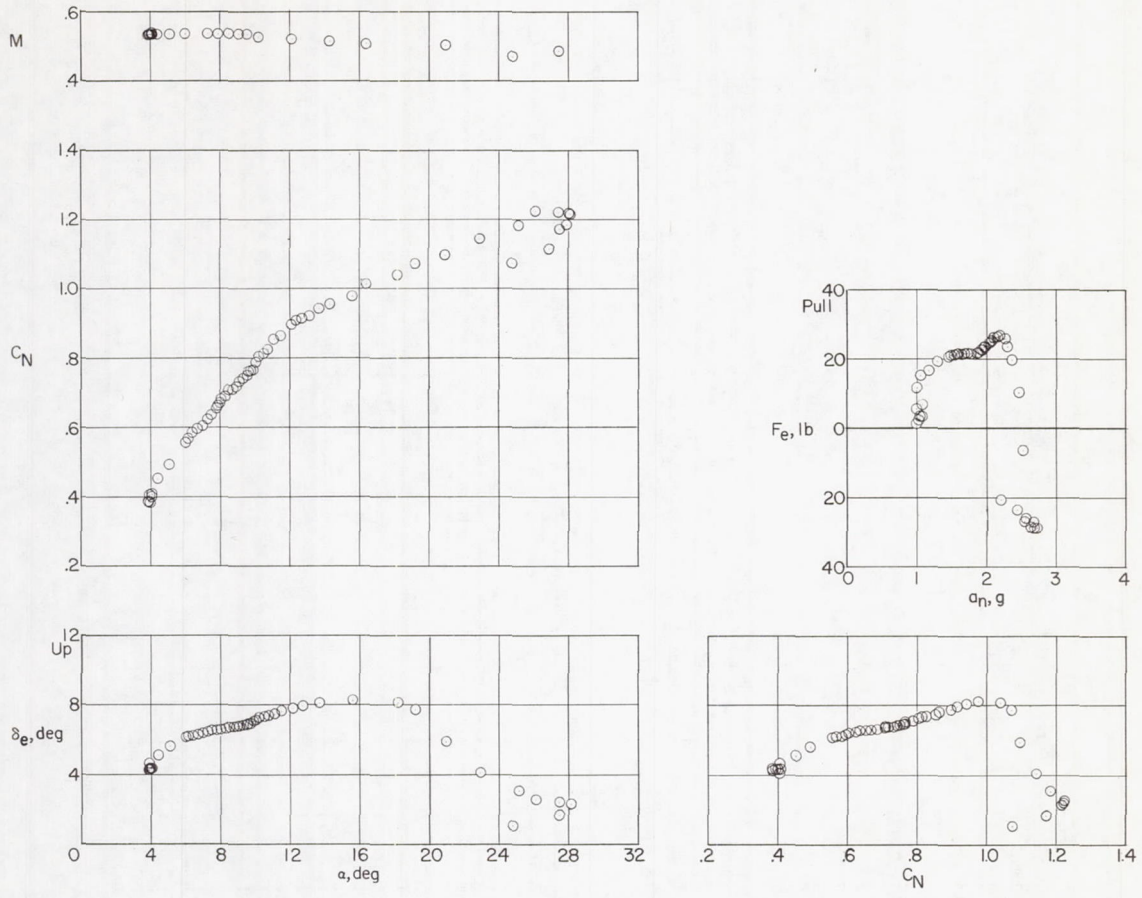

(a) $h_p \approx 23{,}300$ feet; $i_t = 2.2^o$; center of gravity at $0.259\bar{c}$; slats retracted.

Figure 10.- Static longitudinal stability characteristics of the Douglas D-558-II research airplane in turning flight. Inboard wing-fence configuration.

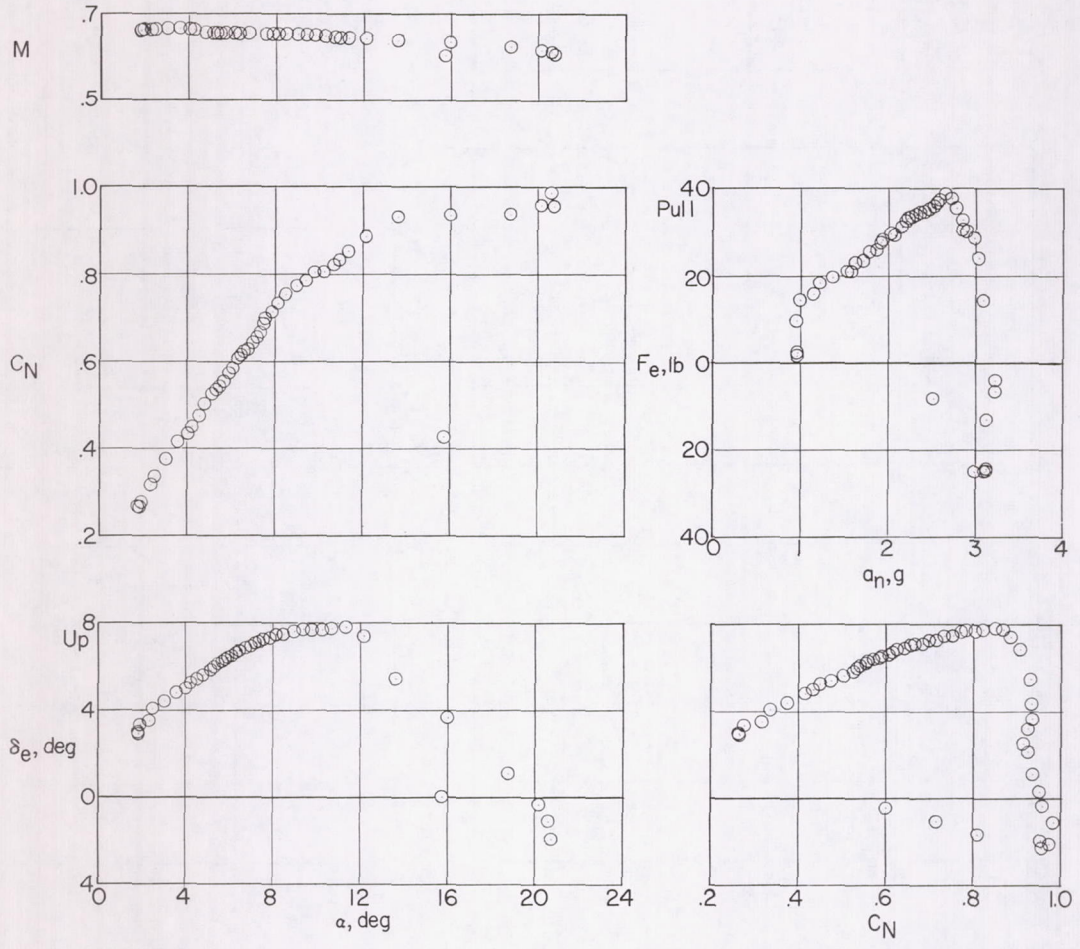

(b) $h_p \approx 25{,}500$ feet; $i_t = 2.3^\circ$; center of gravity at $0.258\bar{c}$; slats retracted.

Figure 10.- Continued.

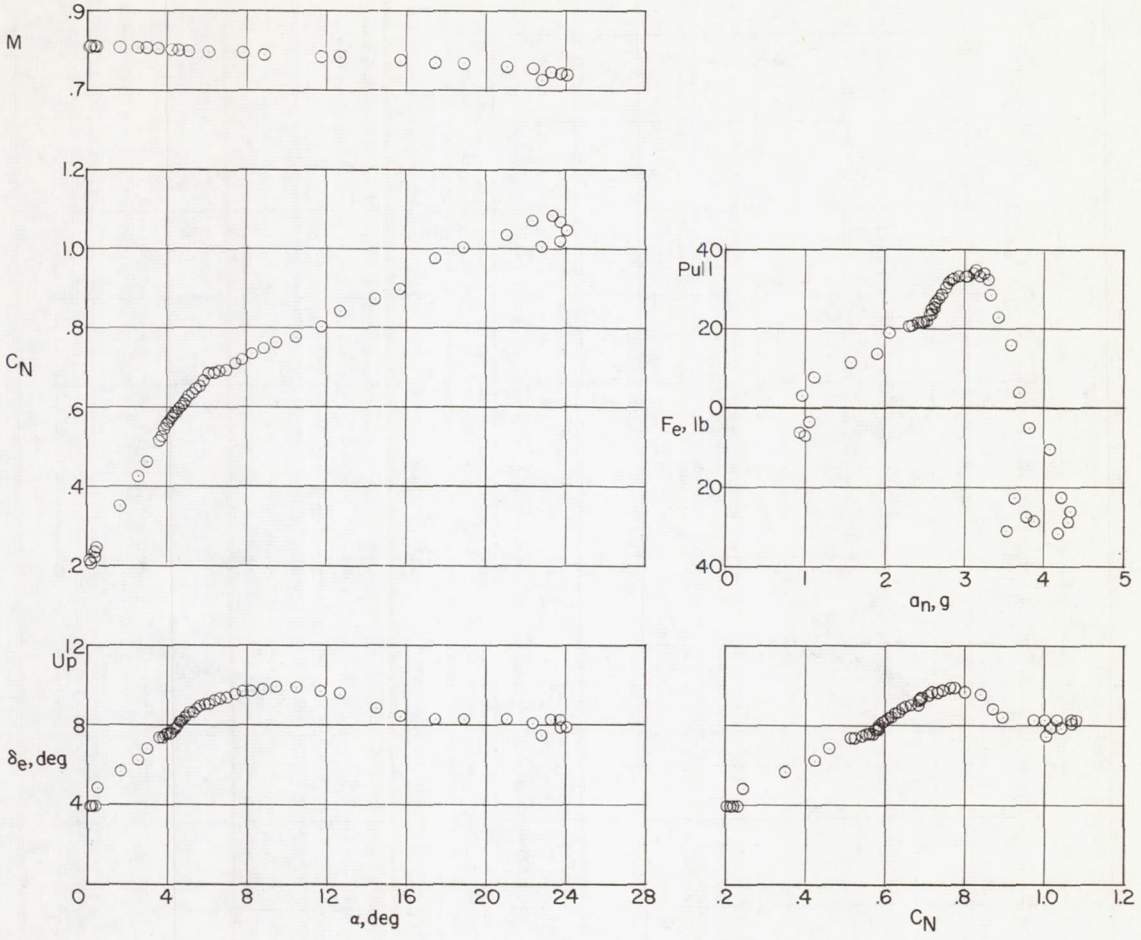

(c) $h_p \approx 28{,}700$ feet; $i_t = 2.0^\circ$; center of gravity at $0.253\bar{c}$; slats retracted.

Figure 10.- Continued.

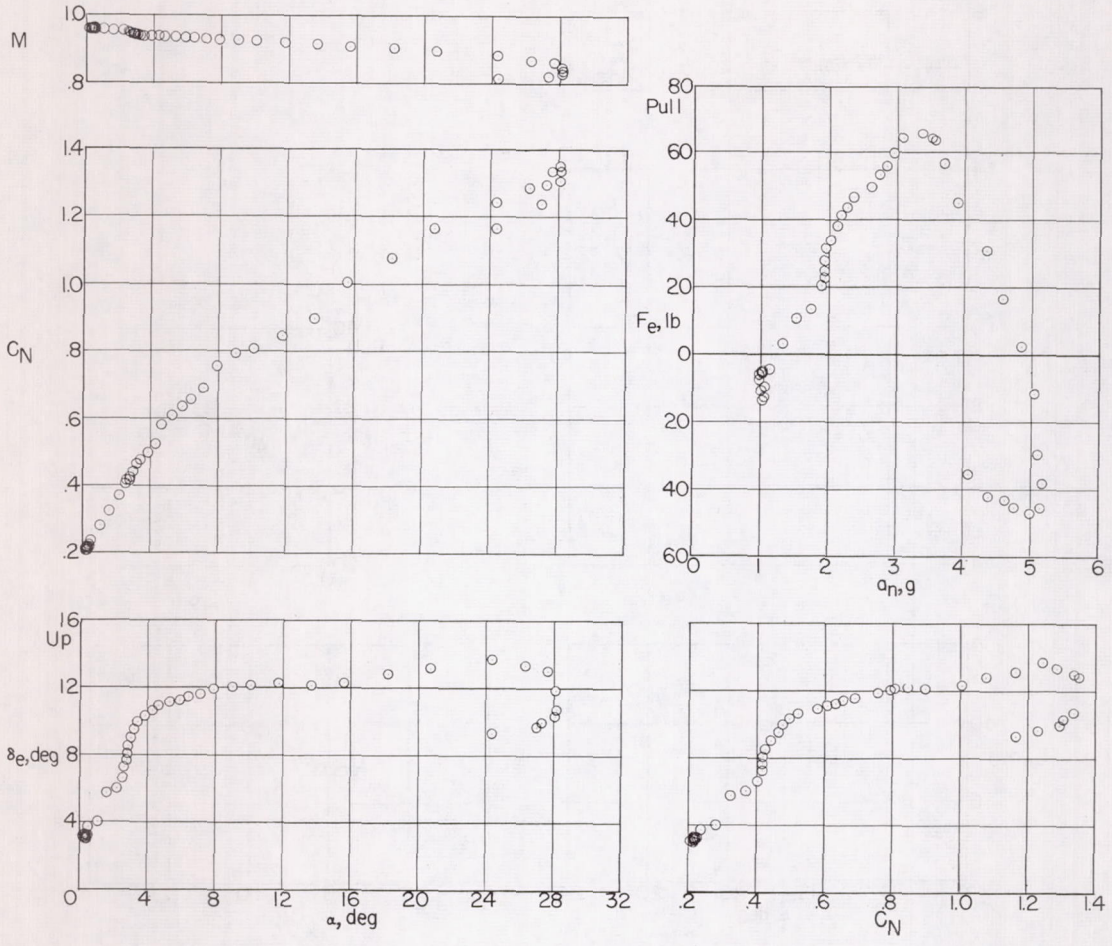

(d) $h_p \approx 34{,}800$ feet; $i_t = 1.6^\circ$; center of gravity at $0.261\bar{c}$; slats retracted.

Figure 10.- Continued.

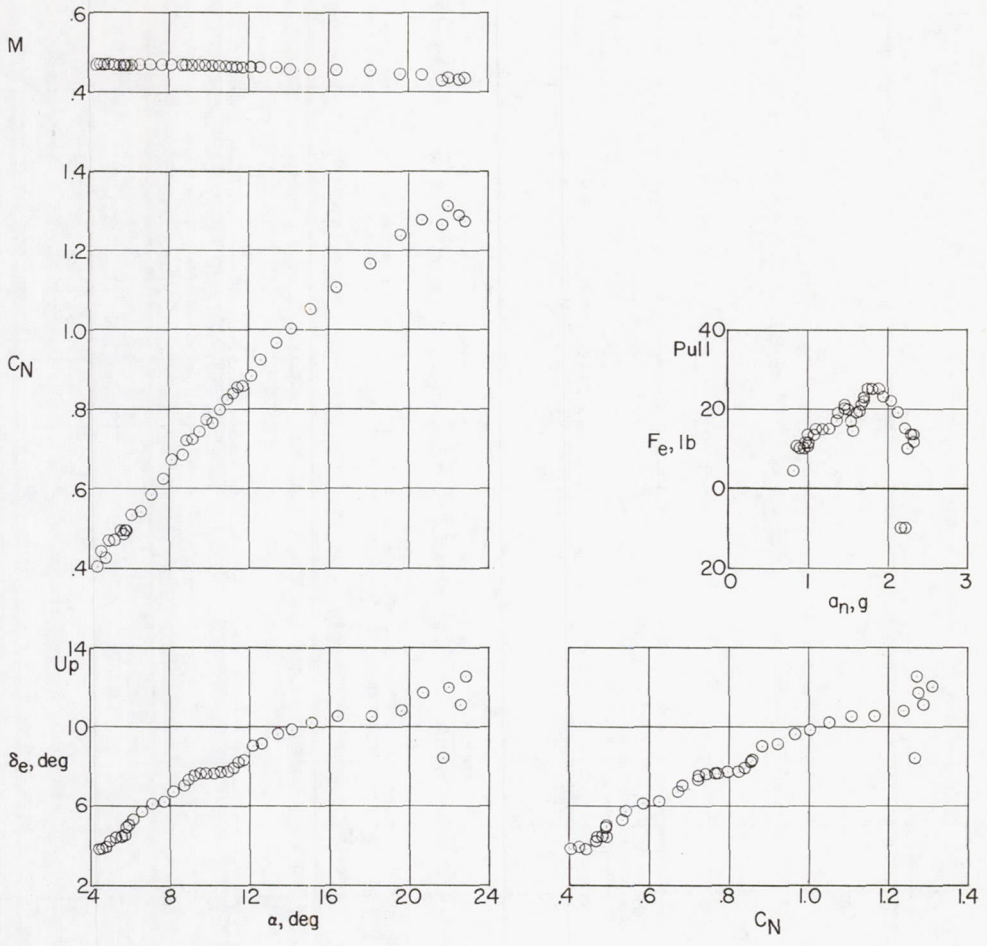

(e) $h_p \approx 22{,}700$ feet; $i_t = 2.1^\circ$; center of gravity at $0.25\bar{c}$; slats unlocked.

Figure 10.- Continued.

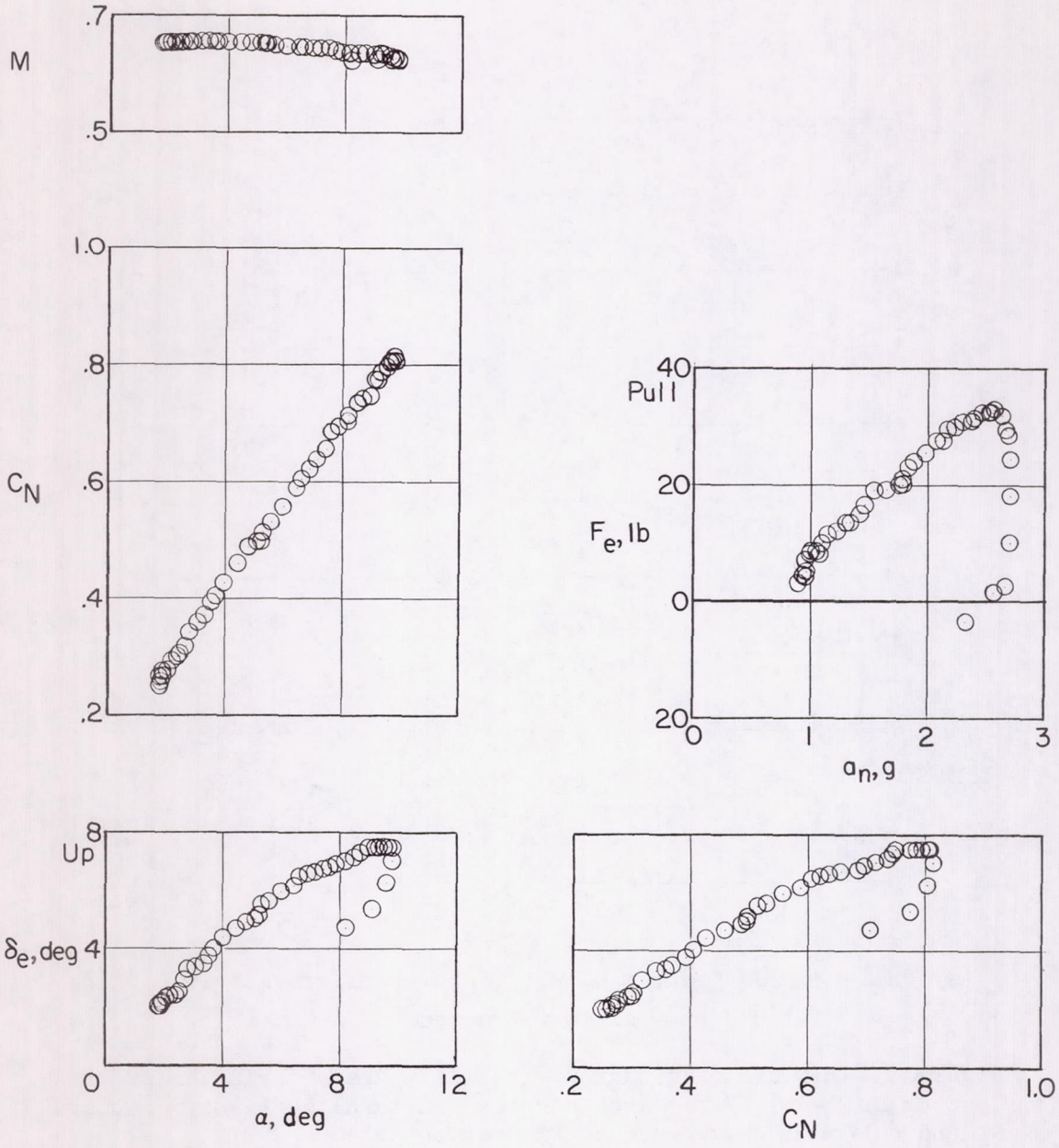

(f) $h_p \approx 24{,}500$ feet; $i_t = 2.1^\circ$; center of gravity at $0.25\bar{c}$; slats unlocked.

Figure 10.- Concluded.

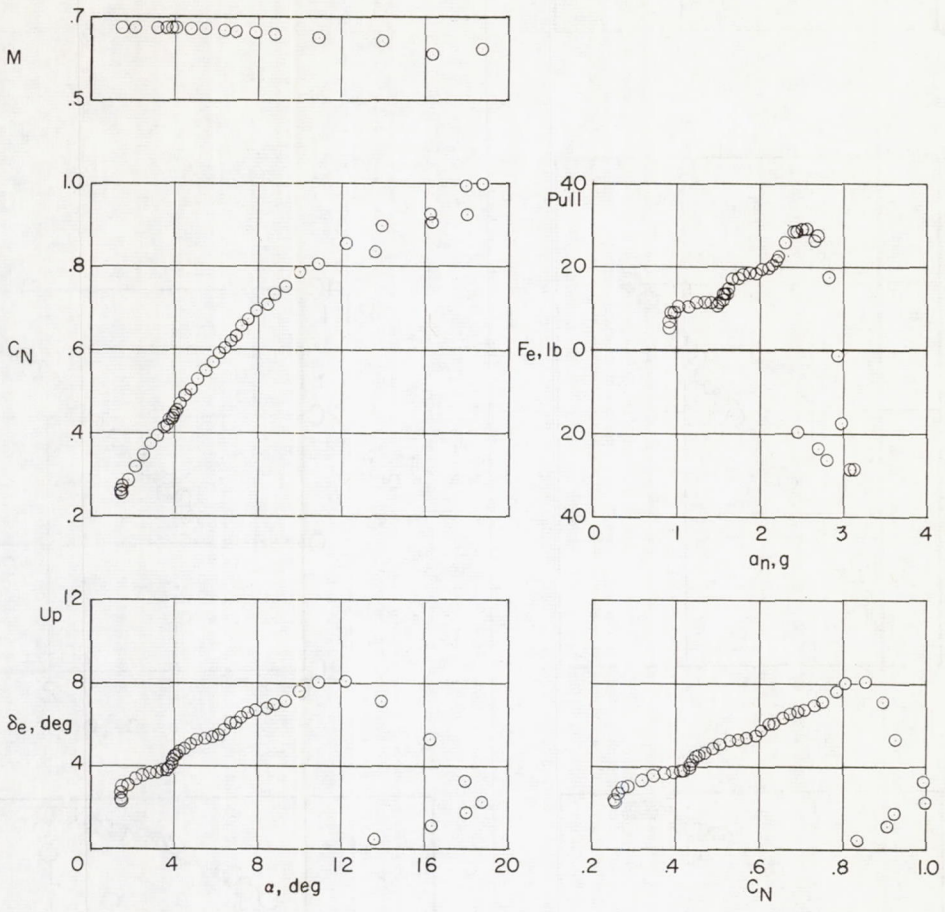

(a) $h_p \approx 26{,}200$ feet; $i_t = 2.1^\circ$; center of gravity at $0.261\bar{c}$; slats retracted.

Figure 11.- Static longitudinal stability characteristics of the Douglas D-558-II research airplane in turning flight. Inboard and outboard wing-fence configuration.

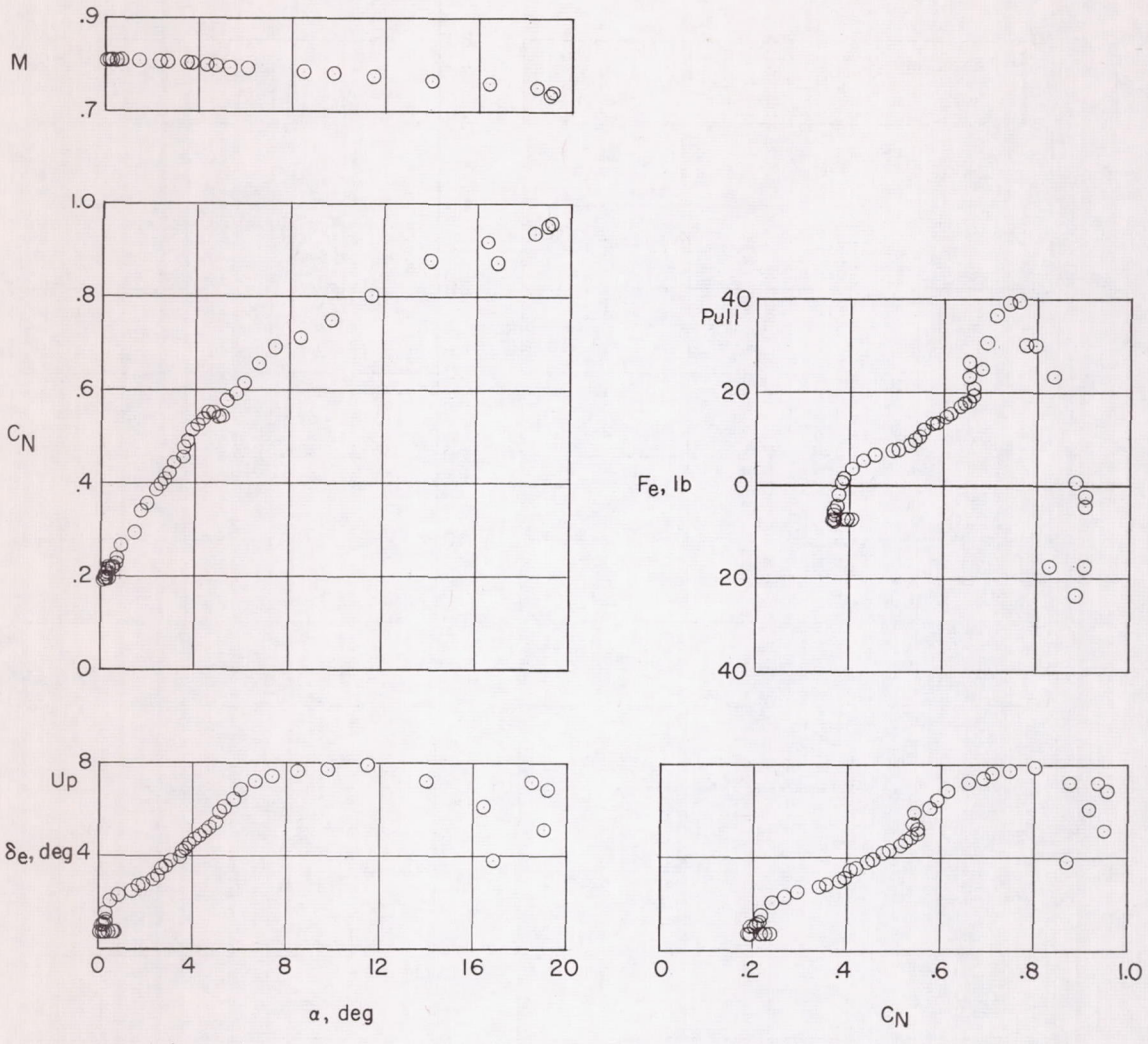

(b) $h_p \approx 30,400$ feet; $i_t = 2.1^\circ$; center of gravity at $0.260\bar{c}$; slats retracted.

Figure 11.- Continued.

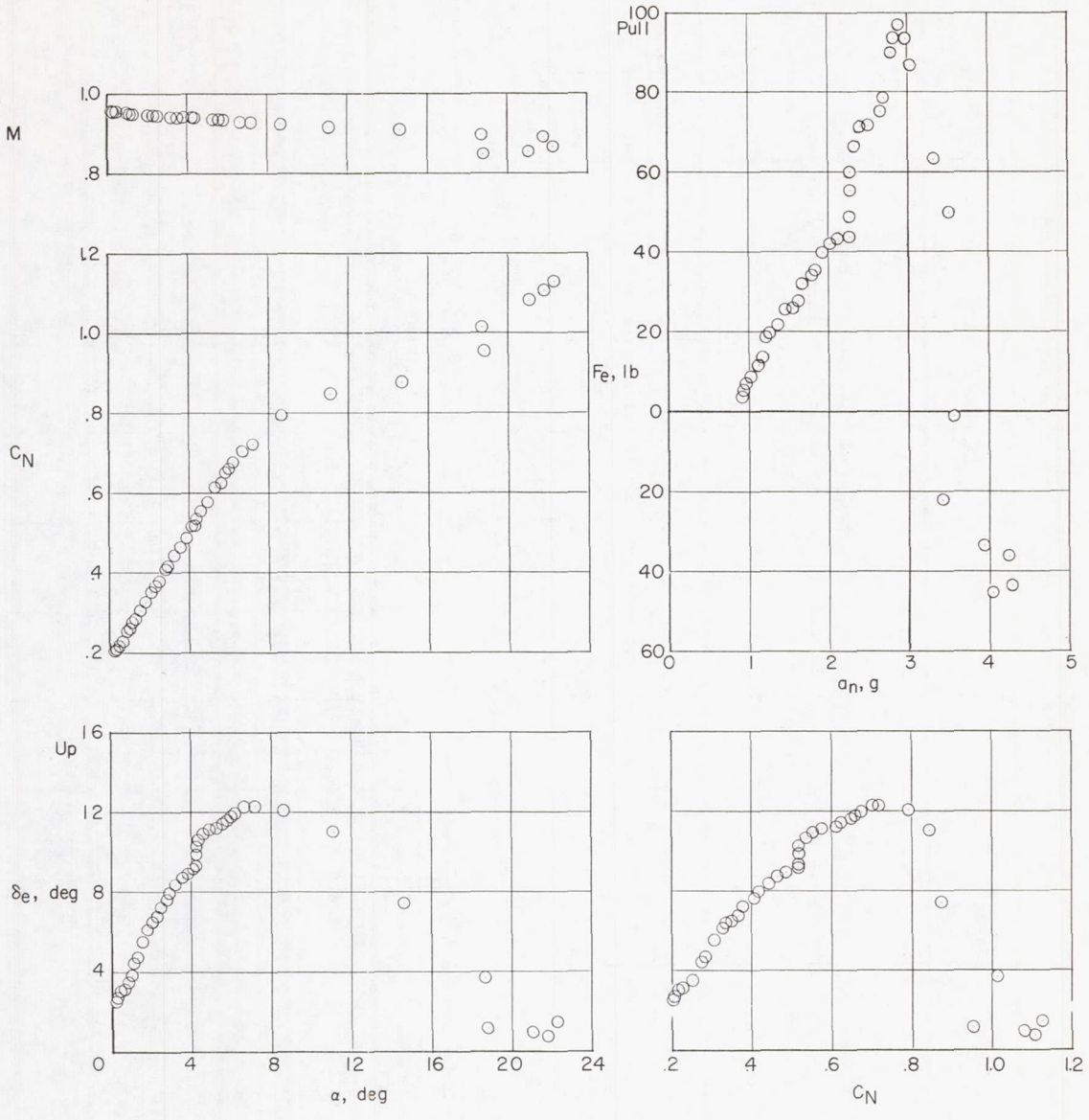

(c) $h_p \approx 35{,}600$ feet; $i_t = 2.1^\circ$; center of gravity at $0.248\bar{c}$; slats retracted.

Figure 11.- Continued.

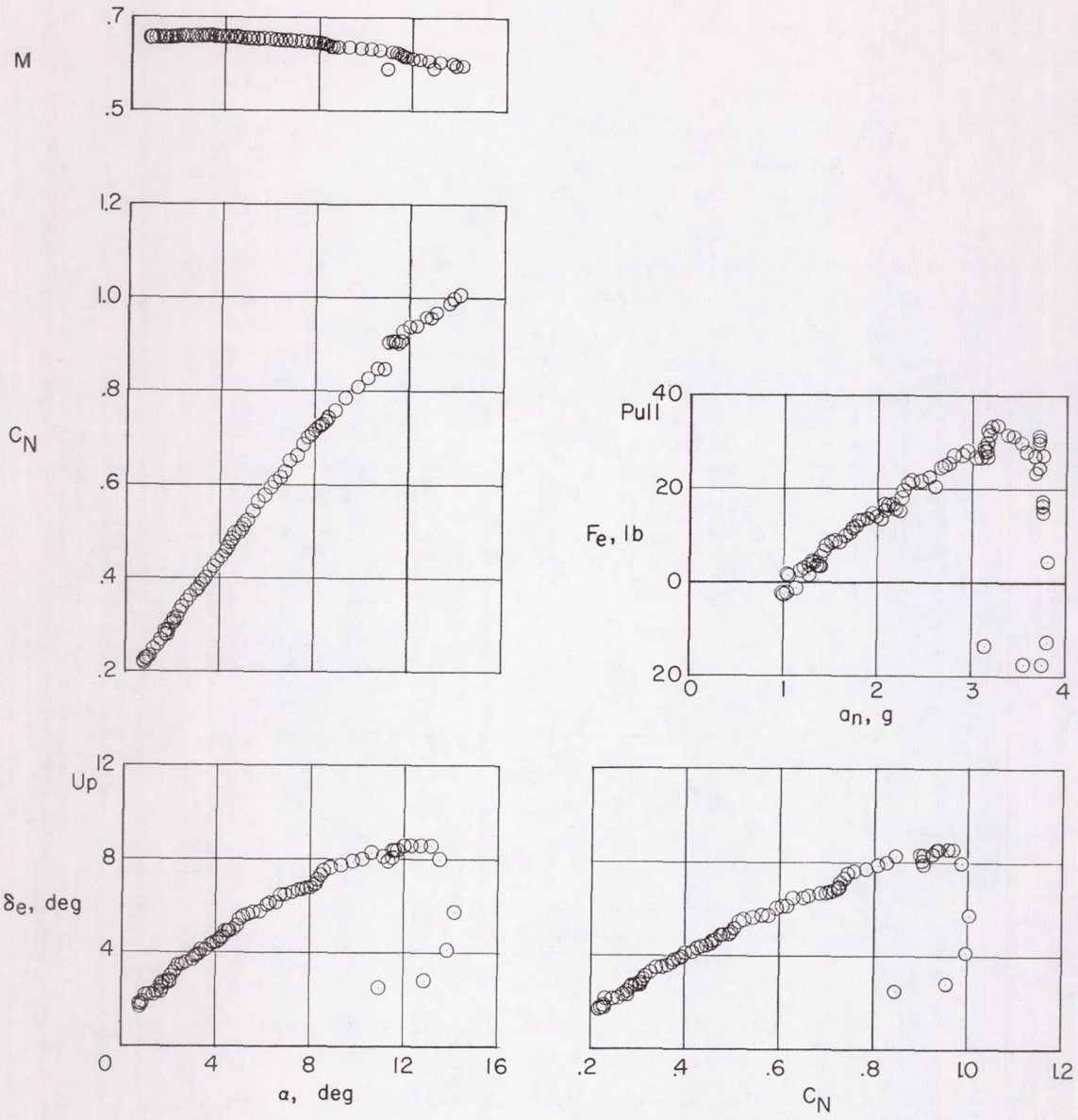

(d) $h_p \approx 20{,}200$ feet; $i_t = 2.3^\circ$; center of gravity at $0.266\bar{c}$; slats unlocked.

Figure 11.- Concluded.

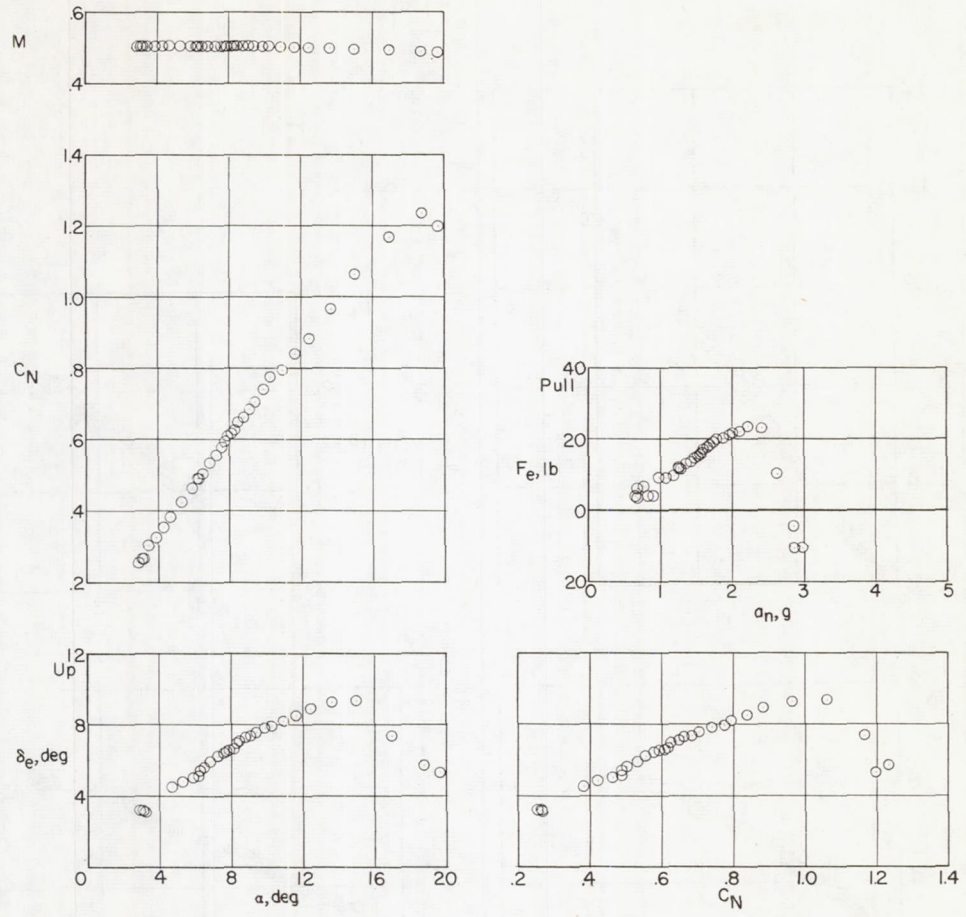

(a) $h_p \approx 20{,}700$ feet; $i_t = 1.6^\circ$; center of gravity at $0.253\bar{c}$.

Figure 12.- Static longitudinal stability characteristics of the Douglas D-558-II research airplane in turning flight. Wing slats fully extended; no wing fences.

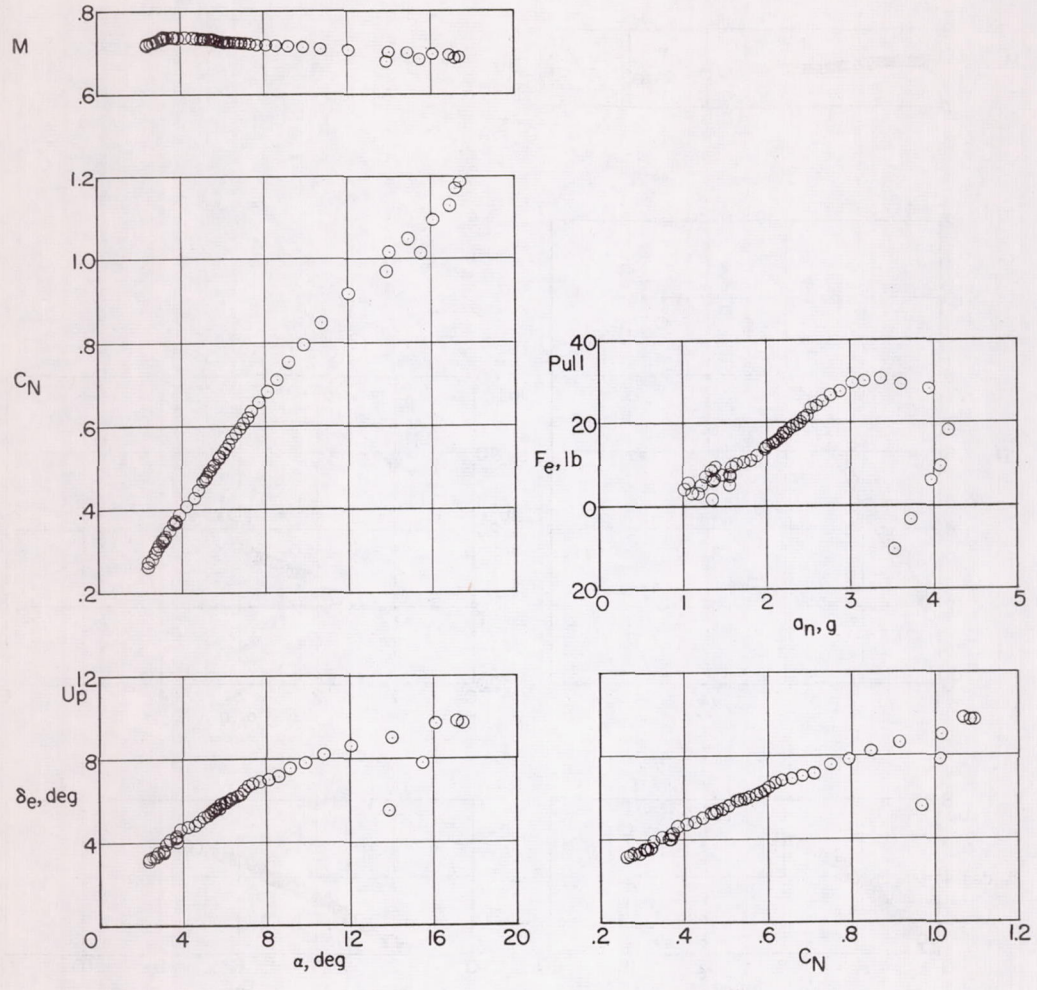

(b) $h_p \approx 26{,}500$ feet; $i_t = 1.6^\circ$; center of gravity at $0.252\bar{c}$.

Figure 12.- Continued.

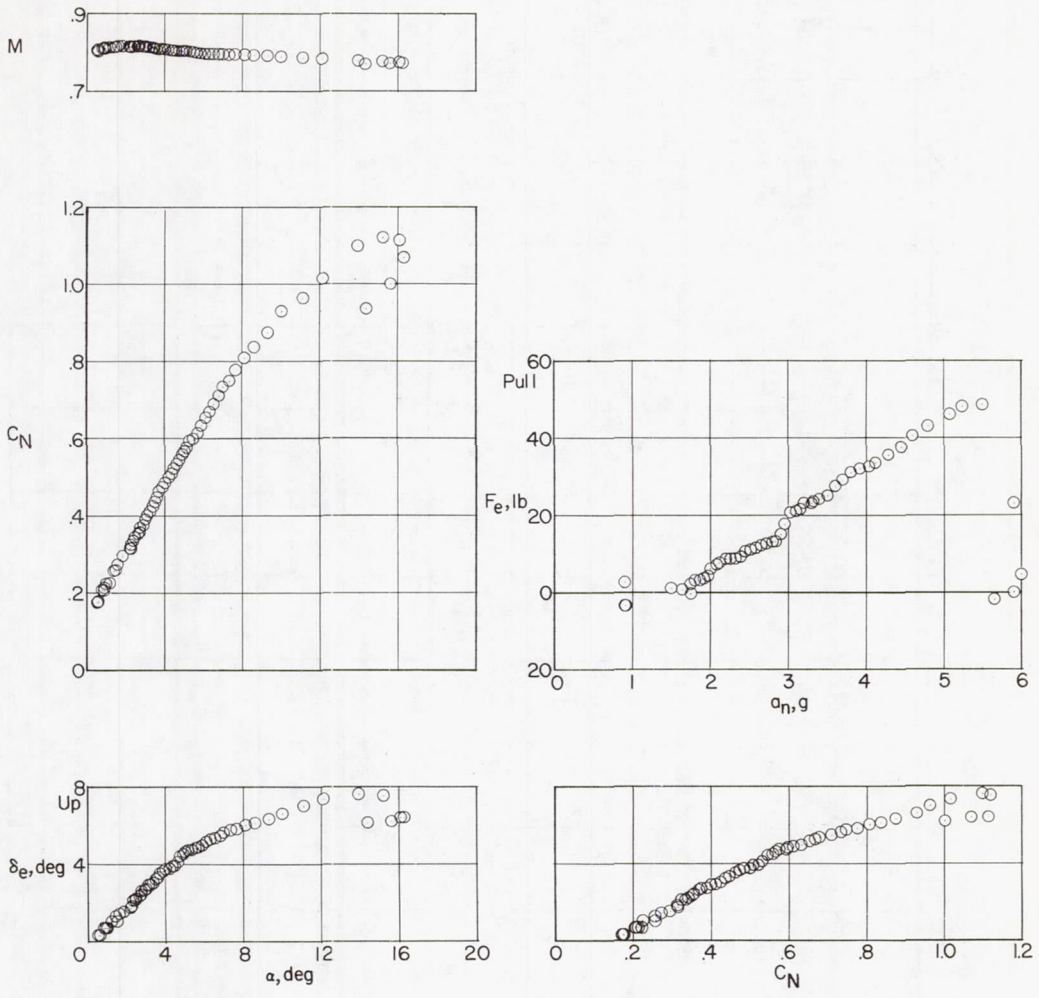

(c) $h_p \approx 23{,}000$ feet; $i_t = 1.3^\circ$; center of gravity at $0.262\bar{c}$.

Figure 12.- Continued.

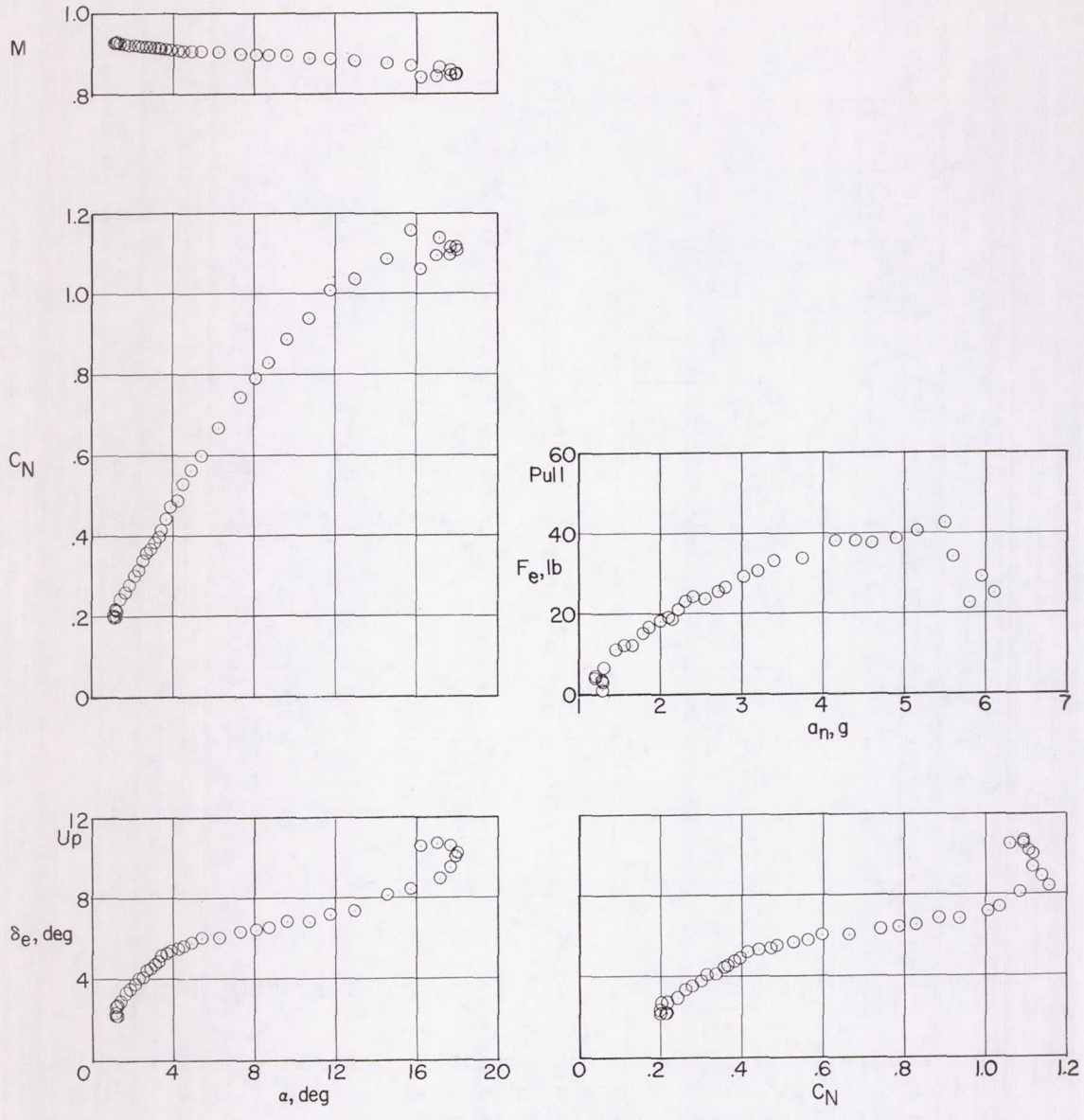

(d) $h_p \approx 27{,}000$ feet; $i_t = 1.3^\circ$; center of gravity at $0.265\bar{c}$.

Figure 12.- Concluded.

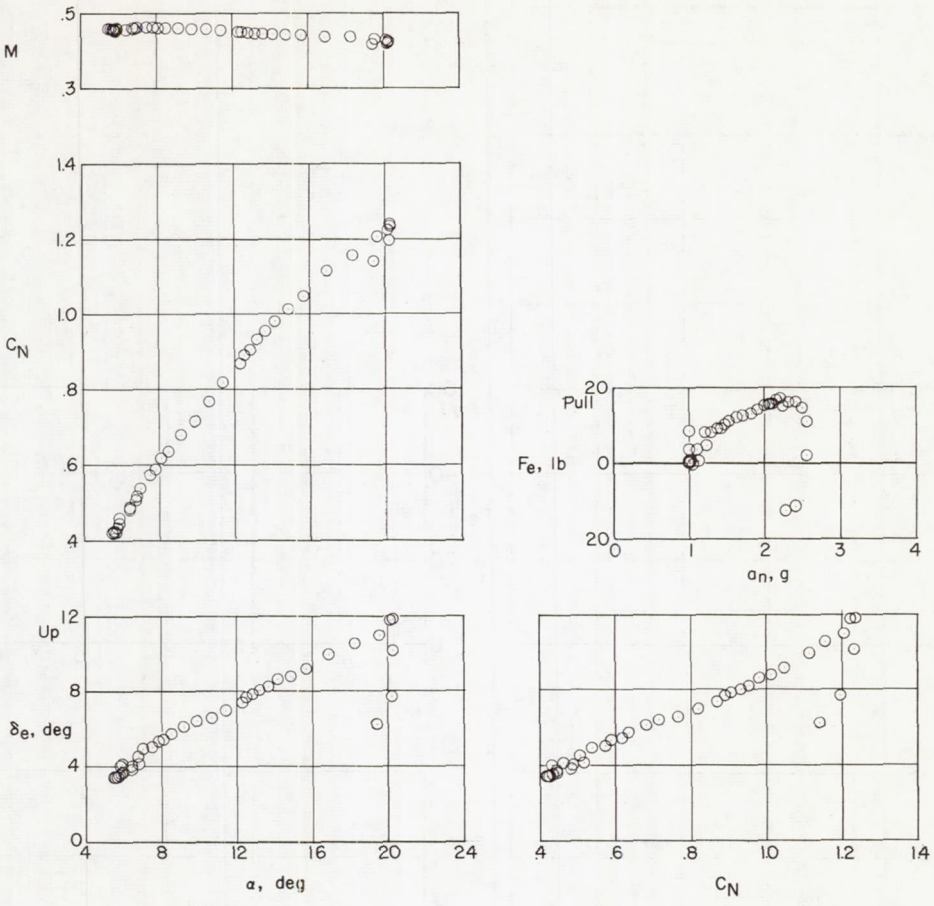

(a) $h_p \approx 18{,}300$ feet; $i_t = 1.6^\circ$; center of gravity at $0.260\bar{c}$.

Figure 13.- Static longitudinal stability characteristics of the Douglas D-558-II research airplane in turning flight. Wing slats fully extended and inboard wing fences.

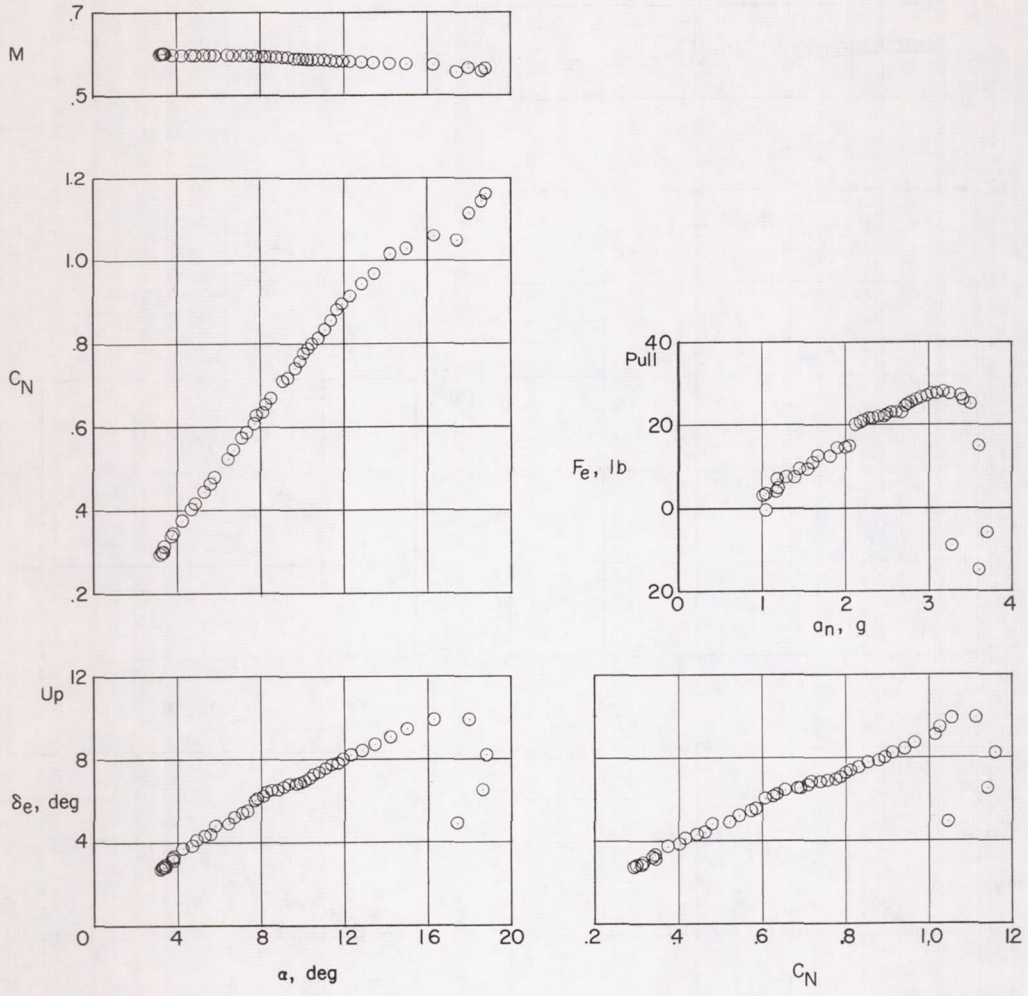

(b) $h_p \approx 21{,}000$ feet; $i_t = 1.6^\circ$; center of gravity at $0.258\bar{c}$.

Figure 13.- Continued.

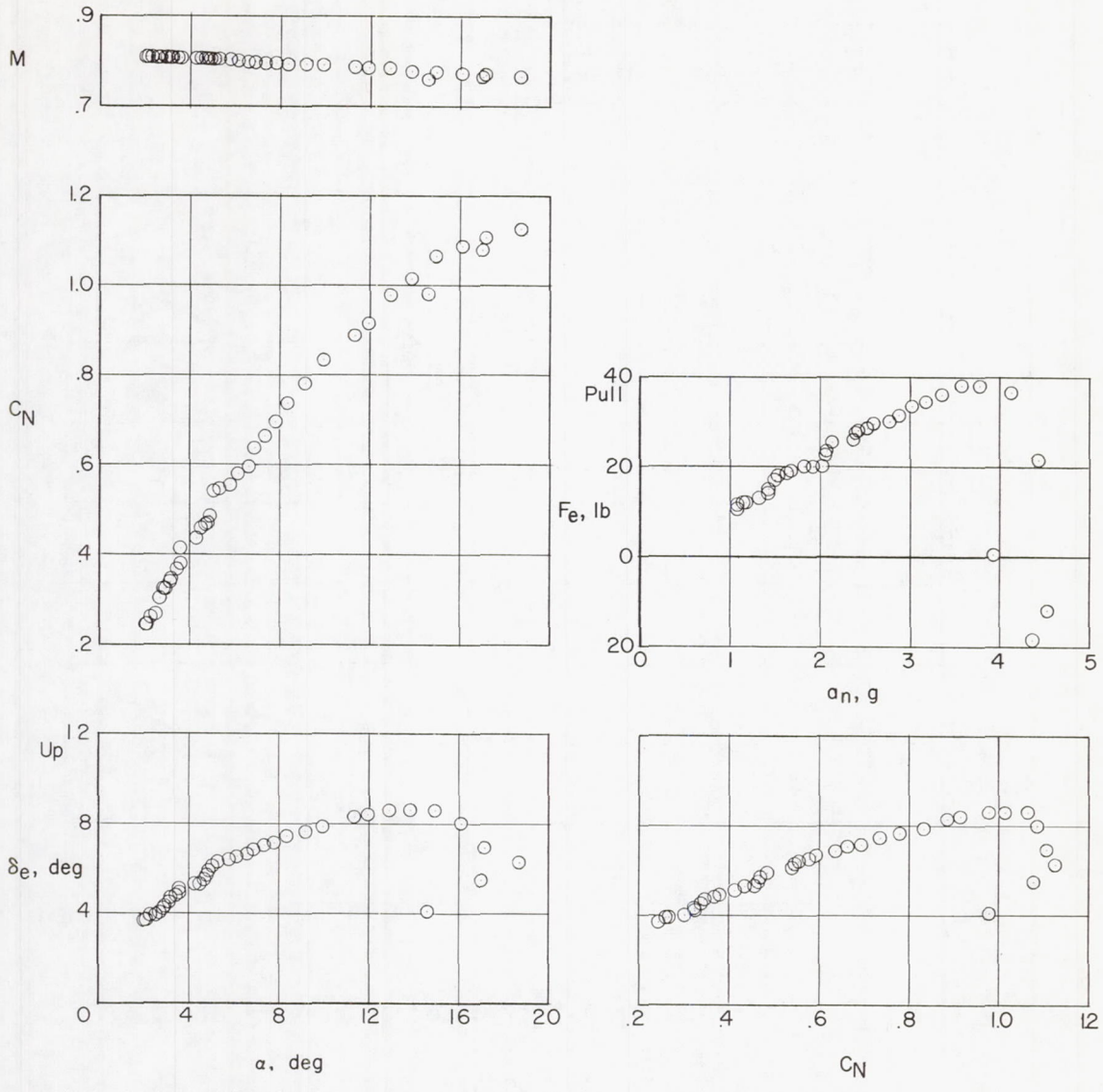

(c) $h_p \approx 28{,}500$ feet; $i_t = 2.3^\circ$; center of gravity at $0.258\bar{c}$.

Figure 13.- Continued.

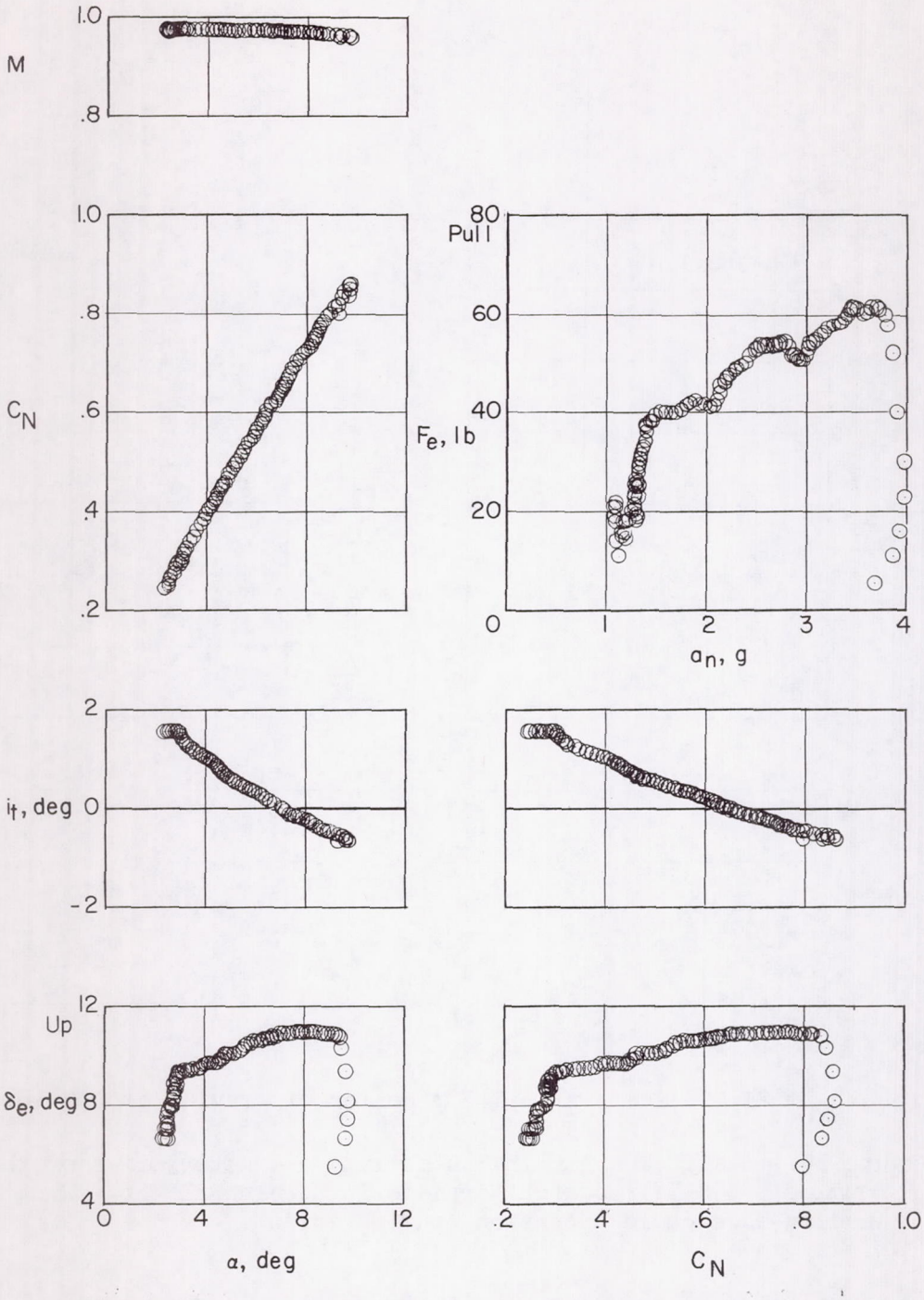

(d) $h_p \approx 35{,}150$ feet; center of gravity at $0.25\bar{c}$.

Figure 13.- Concluded.

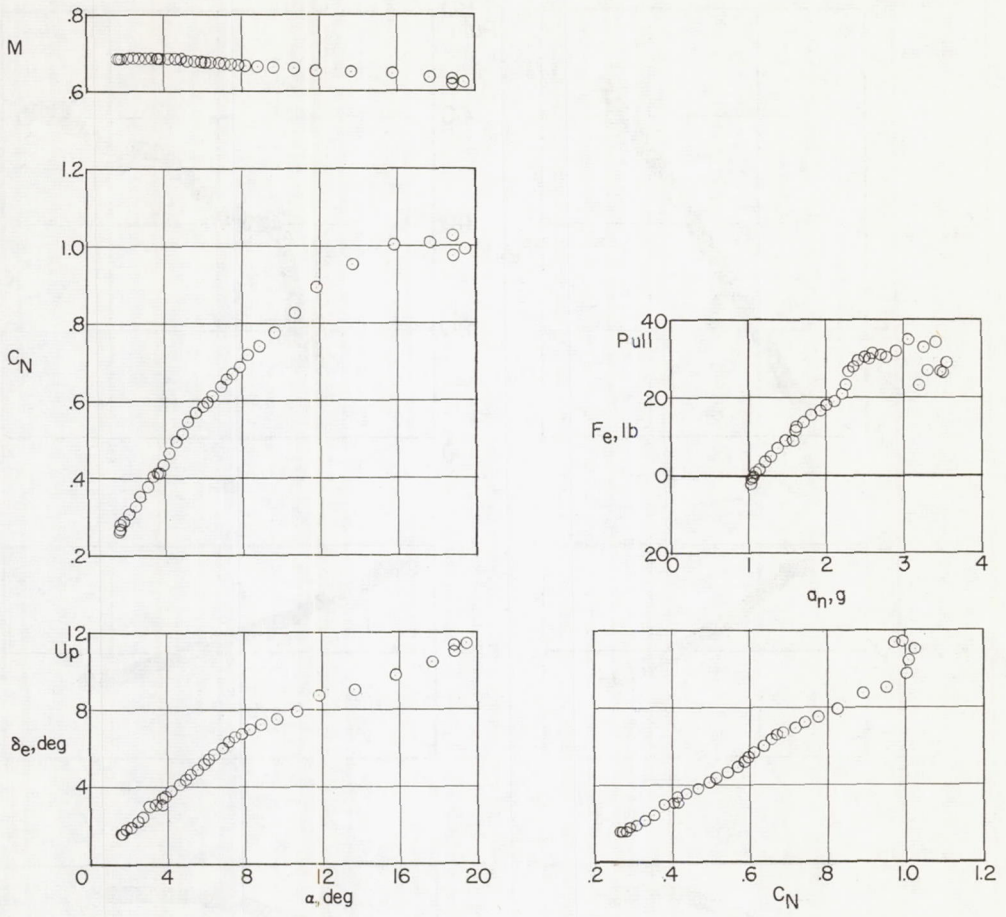

(a) $h_p \approx 23{,}500$ feet; $i_t = 1.7^\circ$; center of gravity at $0.241\bar{c}$.

Figure 14.- Static longitudinal stability characteristics of the Douglas D-558-II research airplane in turning flight. Wing leading-edge chord-extension configuration.

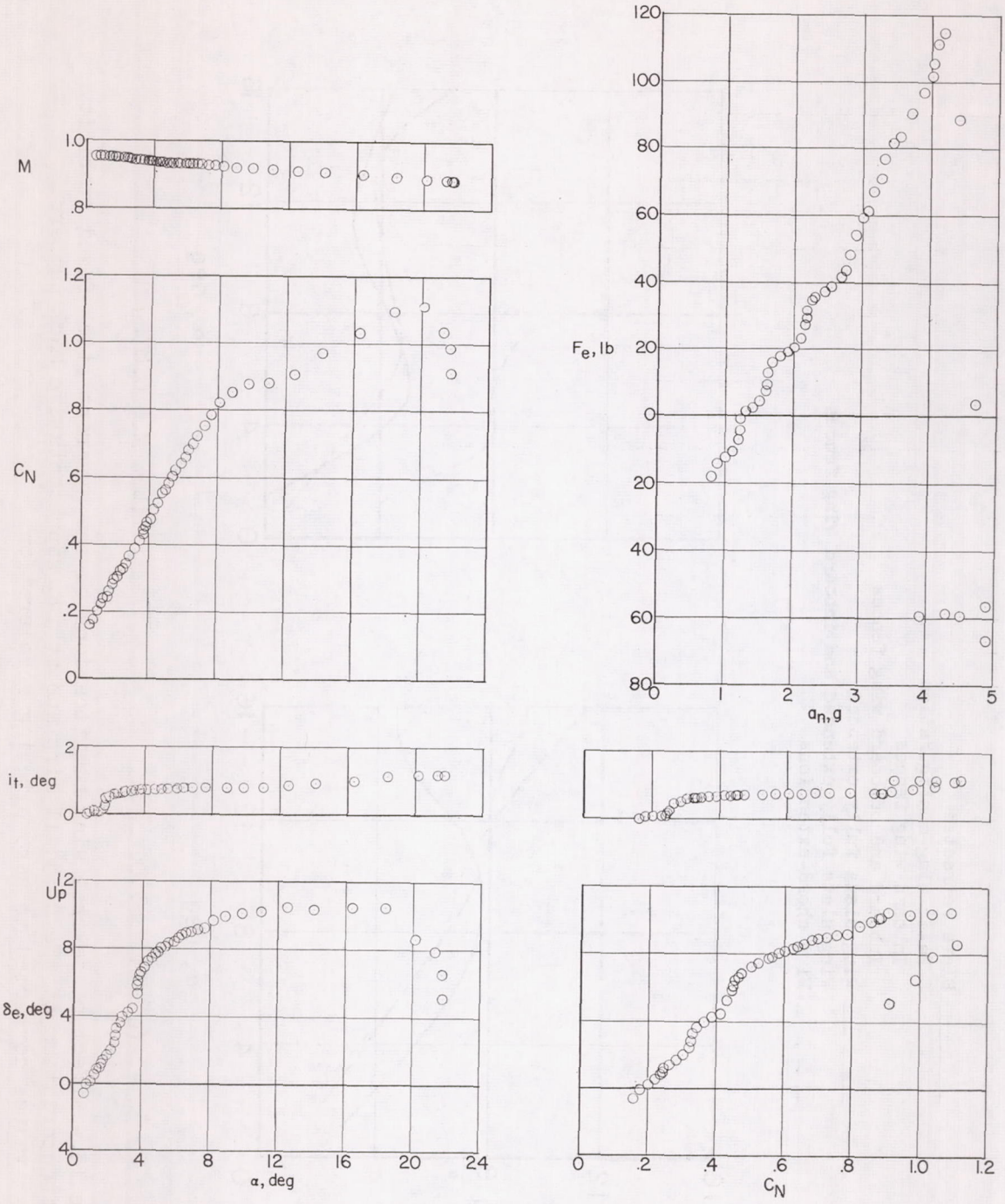

(b) $h_p \approx 32{,}000$ feet; center of gravity at $0.246\bar{c}$.

Figure 14.- Concluded.

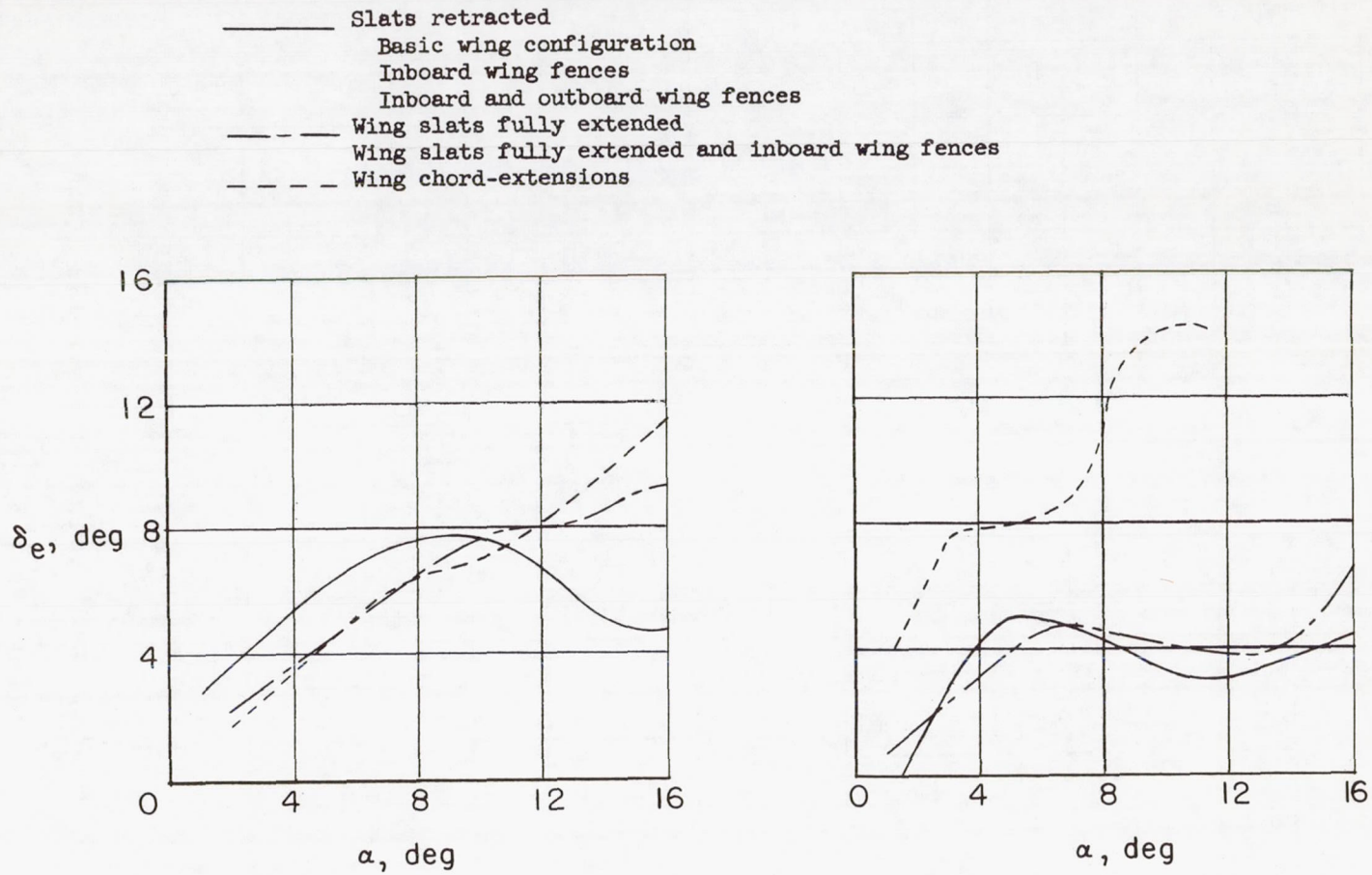

(a) M ≈ 0.70.

(b) M ≈ 0.87.

Figure 15.- Effect of several wing modifications on the apparent stick-fixed stability characteristics of the D-558-II airplane at two representative Mach numbers. (δ_e values corrected to zero pitching acceleration.)

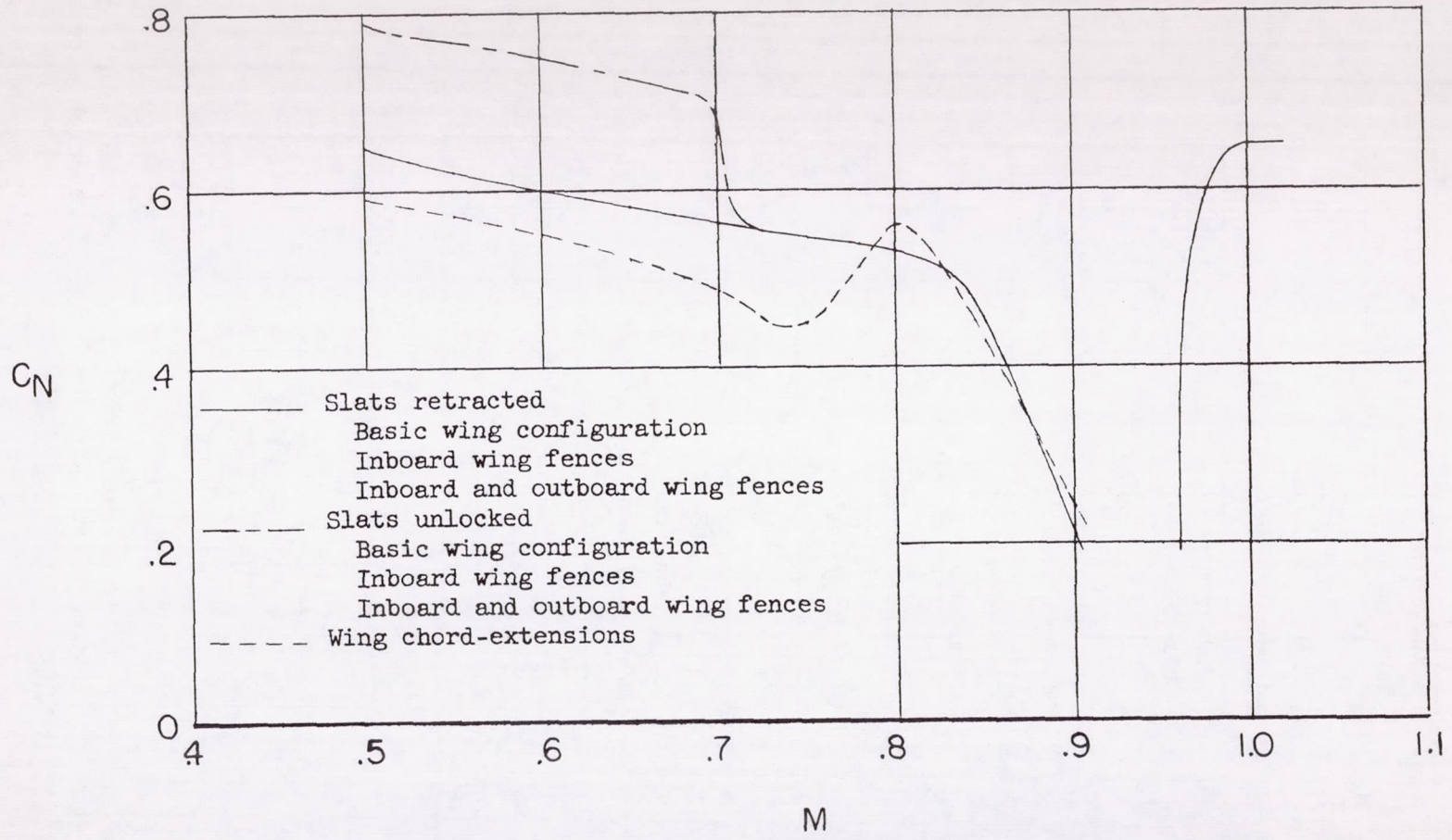

Figure 16.- Effect of wing modifications on buffet boundary of the D-558-II airplane.

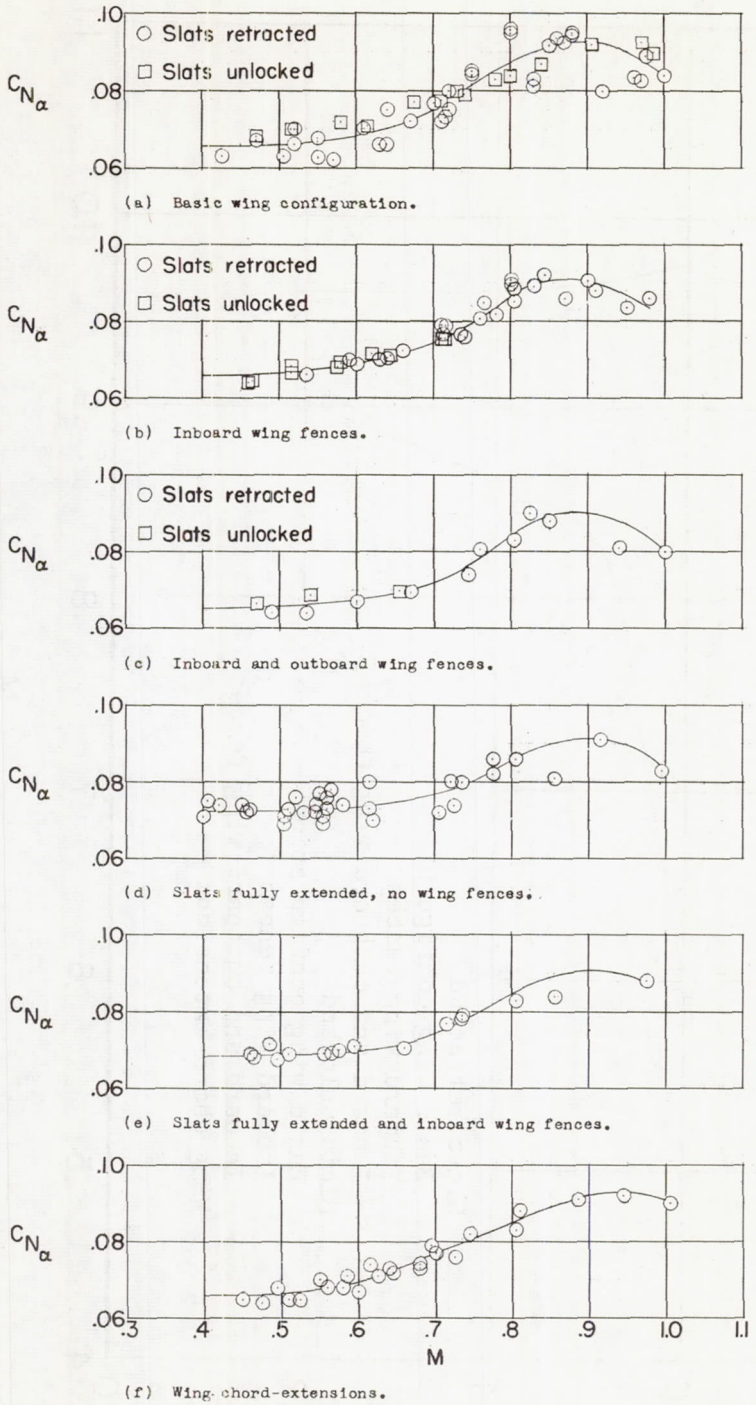

Figure 17.- Effect of several wing modifications on the variation of C_{N_α} with Mach number for the Douglas D-558-II research airplane.

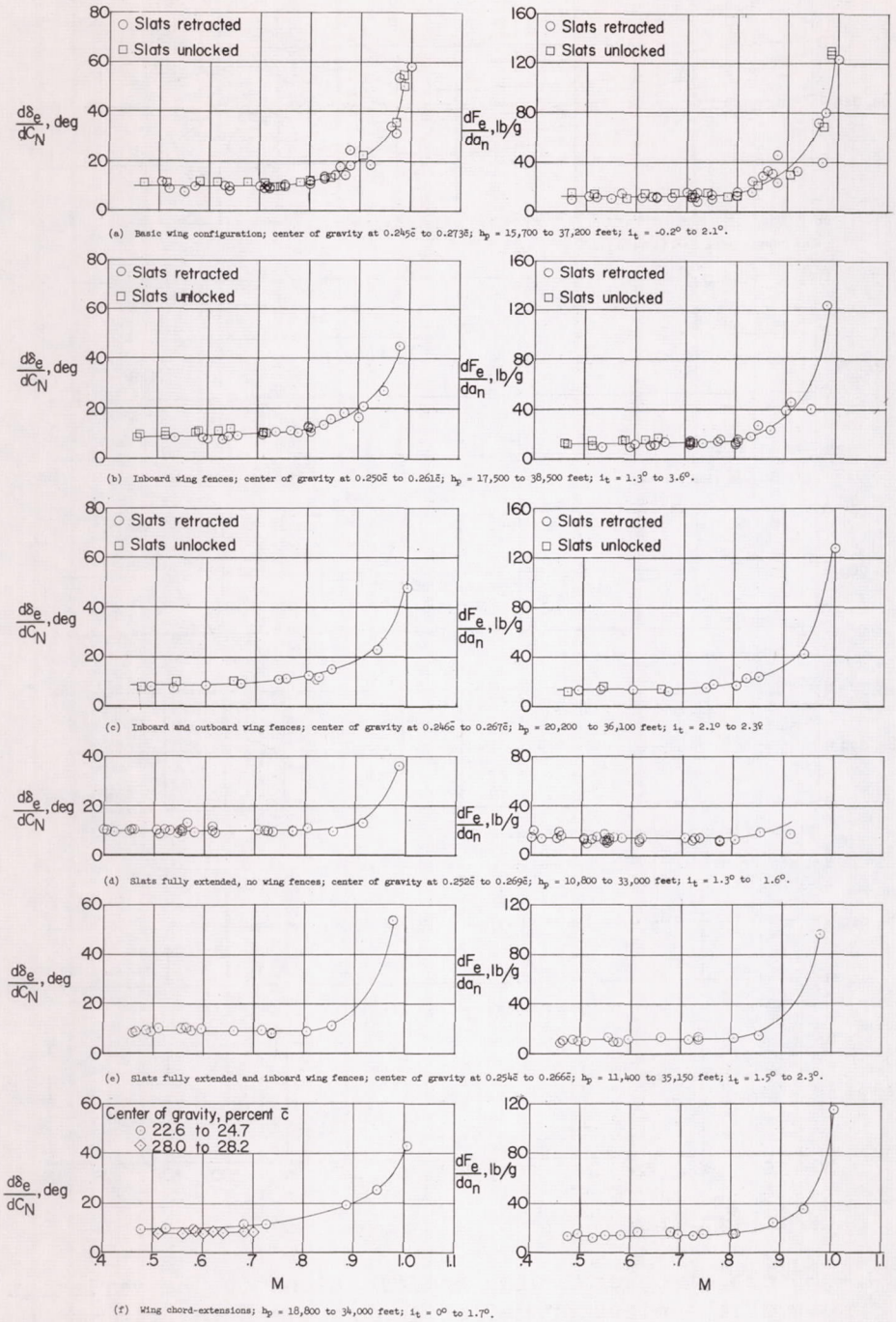

Figure 18.- Effect of several wing modifications on the variation of $d\delta_e/dC_N$ and dF_e/da_n with Mach number for the Douglas D-558-II research airplane.

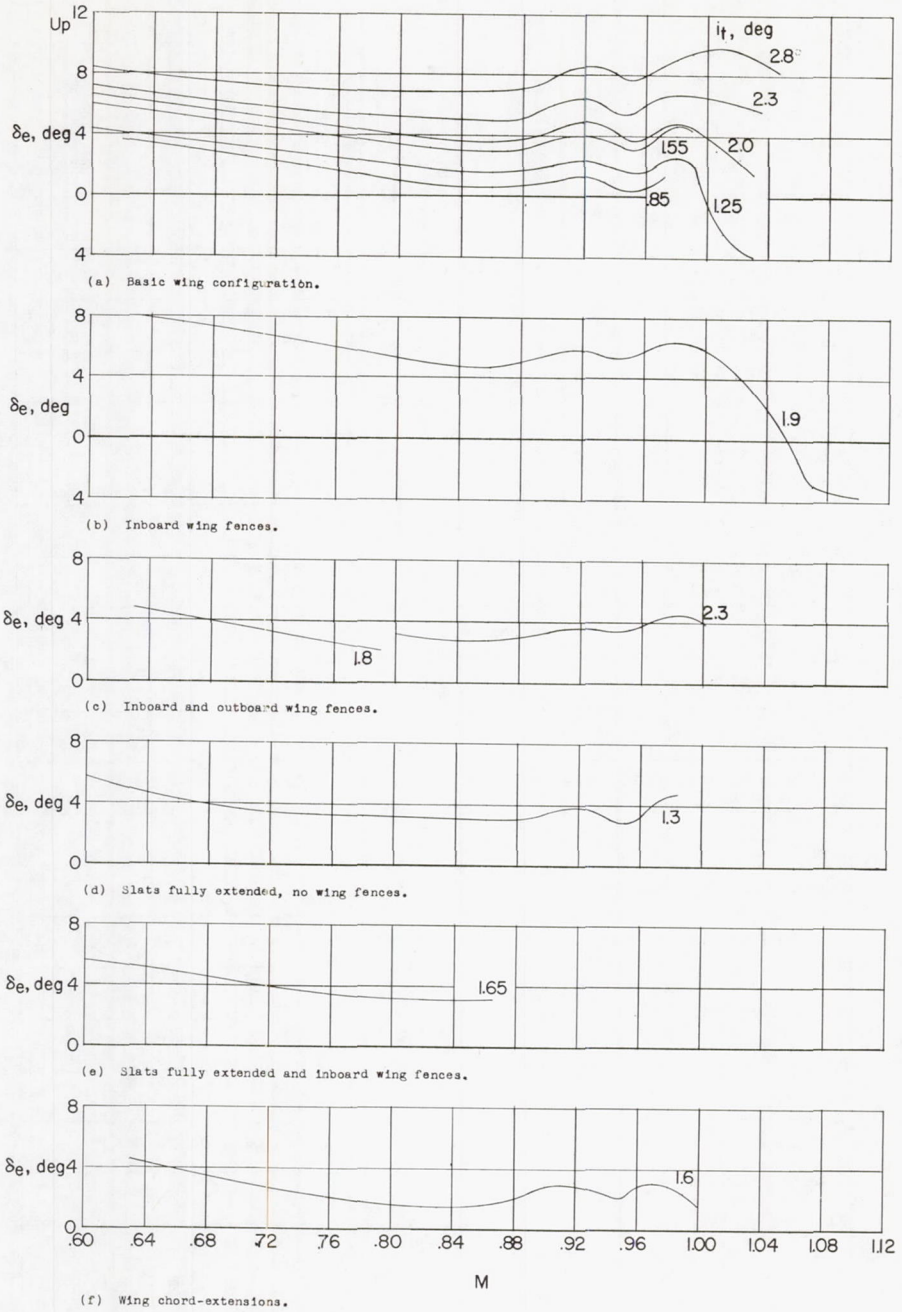

Figure 19.- Effect of several wing modifications on the variation with Mach number of the elevator deflection required to trim the Douglas D-558-II research airplane. h_p = 35,000 feet; W = 13,000 pounds; a_n = 1.

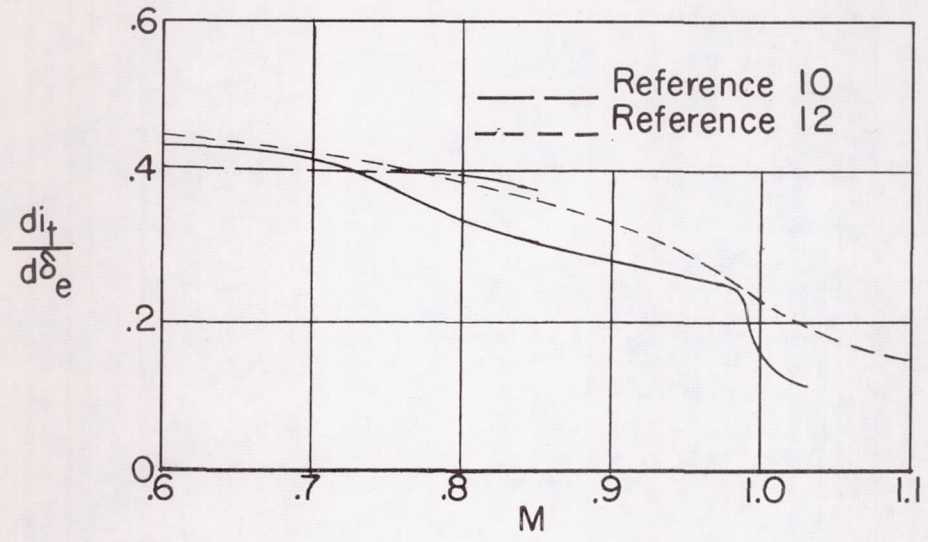

Figure 20.- Variation with Mach number of the relative elevator-stabilizer effectiveness of the Douglas D-558-II research airplane. Basic wing configuration.